Inorganic Chemistry

Article

Cite This: Inorg. Chem. 2019, 58, 2501−2513

pubs.acs.org/IC

Histidine Targeting Heterobimetallic Ruthenium(II)−Gold(I) Complexes

Lucinda K. Batchelor, Daniel Ortiz, and Paul J. Dyson*

Institut des Sciences et Ingénierie Chimiques, Ecole Polytechnique Fédérale de Lausanne (EPFL), CH-1015 Lausanne, Switzerland

Supporting Information

ABSTRACT: Inspired by the preferential, allosteric binding of RAPTA-T and auranofin to the nucleosome core particle , we describe the design and synthesis of a series of heterobimetallic ruthenium(II)−gold(I) complexes with varying spacer lengths ranging from four to eight polyethylene glycol units. Evaluation of their cytotoxicity reveals IC_{50} values in the low micromolar range against cisplatin sensitive and resistant human ovarian carcinoma (A2780, A2780cisR) and nontumoral human embryonic kidney (HEK293) cell lines. Binding studies monitored via mass spectrometry revealed an affinity for histidine residues on a fragment of the amyloid β-protein (residues 1−16, employed as a model system), which is in accordance with the binding sites of parent drugs, RAPTA-C and auranofin, to the nucleosome core particle.

INTRODUCTION

Understanding and controlling the targets of metal-based drugs remains of great importance in the development of selective drugs.[1,2] Ruthenium-based drugs possess a plethora of targets ranging from proteins to DNA,[3,4] and yet directing these complexes toward a desirable target remains challenging. A degree of control can be established in ruthenium(II)-arene complexes by exchanging the bidentate ethylenediamine ligand of $[(\eta^6\text{-}p\text{-cymene})\mathrm{Ru}(\mathrm{en})]\mathrm{PF}_6$ (where *en* = ethylene diamine) (RAED-C) for the compact, water-soluble PTA ligand of $[(\eta^6\text{-}p\text{-cymene})\mathrm{RuCl}_2(\mathrm{PTA})]$ (where PTA = 1,3,5-triaza-7-phosphaadamantane) (RAPTA-C, Figure 1), which directs the complex preferentially toward histone protein binding sites on the nucleosome over those of DNA.[5] Furthermore, DNA binding of RAED-C can be enhanced by substituting the *p*-cymene arene with the more hydrophobic 5,8,9,10-tetrahydroanthracene (THA), resulting in the intercalation of DNA and bimodal binding on naked DNA.[6] On the other hand, RAPTA-C and $[\mathrm{Ru}(\eta^6\text{-toluene})(\mathrm{PTA})\mathrm{Cl}_2]$ (RAPTA-T), which differ only by an iso-propyl group, form specific and identical adducts on histone H2A and H2B histone dimers of the nucleosome core.[7] Notably, a series of binuclear ruthenium(II)-arene complexes are able to cross-link these binding sites, inducing a state of irreversible condensed chromatin, resulting in apoptosis.[8] The binding of RAPTA-T[9] at these sites, consisting of two glutamic acid residues (RU1) and a glutamic acid and histidine residue (RU2), causes a series of structural changes in the nucleosome core that induces a kink in the long α-helix of the H2A histone protein. This structural alteration opens up a binding site for auranofin, a gold(I) drug of the structure (1-thio-β-D-glucopyranose-2,3,4,6-tetraacetato-*S*)-(triethylphosphine)gold(I) (Figure 1), approved for the treatment of rheumatoid arthritis,[10] that is inaccessible prior to the binding of the RAPTA-T. A synergy between the two drugs was discovered where RAPTA-T appears to sensitize the cells to auranofin, resulting in a beneficial increase in tumor cell cytotoxicity and a threefold increase in auranofin chromatin adducts.[11]

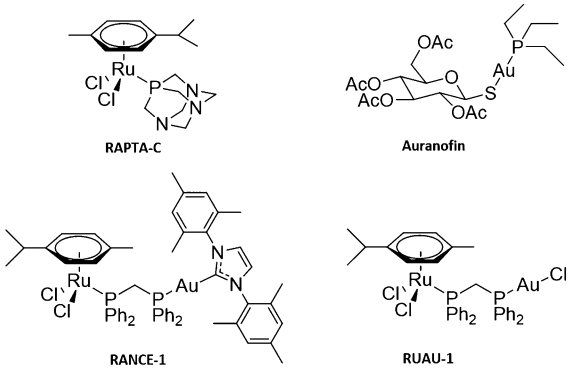

Figure 1. Parent drugs, RAPTA-C and auranofin, and selected heterobimetallic complexes.

Heterobimetallic complexes have emerged as a promising family of complexes that can combine the attributes and targets of two metals within one structure.[12−18] As well as the capacity to possess markedly higher activities than the parent drugs alone,[19] heterometallic drugs have a myriad of potential applications. Numerous heterometallic complexes possessing photophysical properties have been considered for cellular imaging,[20,21] as trackable probes,[22,23] and as drug carriers for cytotoxic complexes.[24−26] Ferrocenyl and titanocene complexes are particularly versatile building blocks for heterometallic complexes due to their facile functionalization and favorable redox properties[27−34]

Received: November 1, 2018
Published: February 7, 2019

DOI: 10.1021/acs.inorgchem.8b03069
Inorg. Chem. 2019, 58, 2501−2513

Scheme 1. Synthesis of Heterobimetallic Ruthenium(II)−Gold(I) Complexes, where n = 4 (a), 5 (b), 6 (c), and 8 (d)

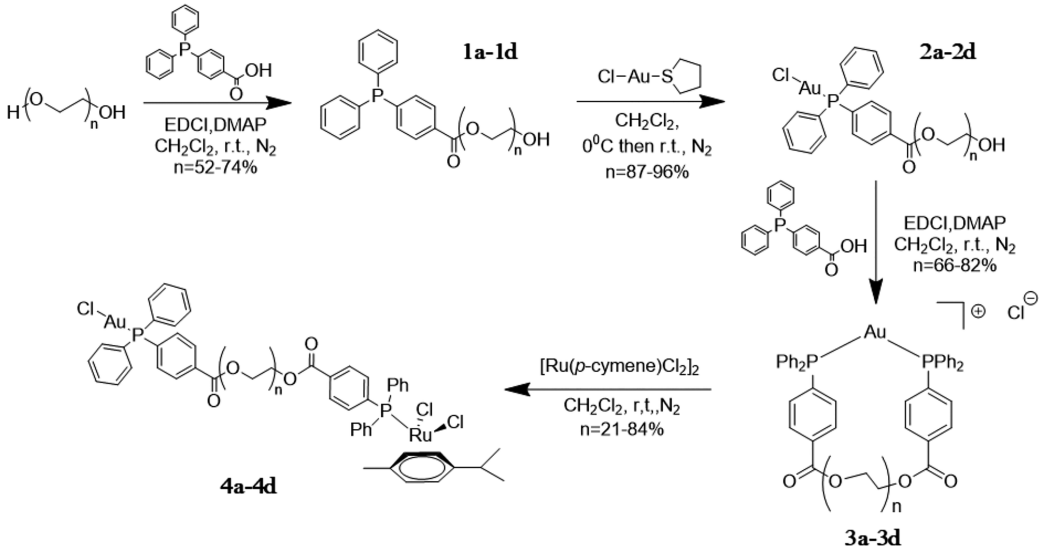

However, heterometallic complexes combining cisplatin-, RAPTA-, and auranofin-type drugs have been scarcely explored. Ruthenium−gold and ruthenium−platinum species have been shown to possess cytotoxicities comparable to cisplatin against HeLa cells.[35] A platinum(II)−gold(I) complex was encapsulated within a ferritin cage with the aim of enhancing its selectivity; however, the complex was unstable with the gold(I) complex binding to the protein and platinum remaining in the bulk, decreasing the efficacy of the agent.[36] A ruthenium(II)−platinum(IV) prodrug possessing high cytotoxicity against cisplatin resistant cells was also able to inhibit cell migration.[37]

The combination of RAPTA complexes, which possess a general low toxicity and antimetastatic properties,[2] and auranofin, which is highly cytotoxic with anti-inflammatory properties,[38] offers great potential. Few heterometallic complexes based on ruthenium(II)-arene compounds and auranofin have been reported. $[(\eta^6\text{-}p\text{-Cymene})RuCl_2(\mu\text{-dppm})Au(IMes)]ClO_4$ (RANCE-1, Figure 1), where dppm = diphenylphophanylmethyl(diphenyl) phosphane and IMes = 1,3-bis(2,4,6-trimethylphenyl)imidazole-2-ylidene), is a promising heterobimetallic complex exhibiting efficient inhibition of thioredoxin reductase (TrX), vascular endothelial growth factor (VEGF), pan-matrix metalloproteinases (pan-MPP), and pan-cathepsin. When compared to auranofin, RANCE-1 presents similar antiproliferative activity against renal cancer cell line (Caki-1) and improved inhibition of VEGF, pan-MMP, and pan-cathepsin.[39] Replacing the auranofin-like thiolato-β-D-glucose tetraacetate ligand with a chloride ligand results in a threefold decrease in cytotoxicity against human ovarian carcinoma (A2780) cells.[40] Other examples include $[(\eta^6\text{-}p\text{-cymene})RuCl_2(\mu\text{-dppm})AuCl]$ (RUAU-1, Figure 1) and $[(\eta^6\text{-}p\text{-cymene})RuCl_2(\mu\text{-dppm})Au(S\text{-thiazoline})]$, which shows that differing the sacrificial ligand coordinated to the gold center does not impact the activity in this case.[41] However, introducing N-heterocyclic carbene ligands to the gold center in cationic ruthenium(II)−gold(I) complexes of the same structure can enhance tumor cell selectivity.[42]

Herein, we describe the synthesis, cytotoxicity, and target binding studies of a series of heterobimetallic complexes containing RAPTA-C− and auranofin-like fragments. The design of the complexes aims to preserve the structure of the parent drugs, RAPTA-C and auranofin, as closely as possible while allowing flexibility to enable binding at two different and distal sites. A series of linker lengths was explored to determine the impact of the linker length on the cytotoxicity of the complexes. The ability of the complexes to bind to histidine residues was explored via mass spectrometry using both single amino acids and a fragment of the amyloid β-protein.

RESULTS AND DISCUSSION

With the aim of targeting the binding sites of RAPTA-C and auranofin, maintaining the key structural features of the parent drugs is important. However, alterations are required in order to tether the complexes via a flexible linker with the PTA and triethylphosphine ligands, belonging to RAPTA-C and auranofin, respectively, being replaced by 4-(diphenylphosphophino)benzoic acid ligands, which provide a functionalizable carboxylic acid moiety and air stability. The labile thio-β-D-glucose-2,3,4,6-tetraacetate ligand of auranofin is replaced with a labile chloride ligand. The p-cymene arene and the two labile chloride ligands present in RAPTA-C were maintained due to the hydrophobic interactions provided by the arene during binding and the vital role of the chlorides in the activation of the complex via aquation. Polyethylene glycol was selected as a suitable linker due to its flexibility and its higher water solubility compared to that of alkyl chains.

As a 4-(diphenylphosphophino)benzoic acid ligand is coordinated to both the ruthenium(II) and the gold(I) centers, care must be taken to achieve high selectivity in the coupling step. Manipulation of reaction stoichiometry was insufficient to control the monocoordination of either ruthenium or gold to a bis-phosphine ligand. Therefore, monophosphine ligands (**1a−1d**) were prepared via the esterification reaction between 1 equiv of 4-(diphenylphosphophino)benzoic acid and 1.5 equiv of the appropriate polyethylene glycol chain using *N*-ethyl-*N*′-(3-dimethlaminopropyl)carbodiimide hydrochloride (EDCI) as coupling reagent and 4-(dimethylamino)pyridine (DMAP) as base catalyst (Scheme 1). Ligands **1a−1d** (Scheme 1) were coordinated to the gold via a freshly prepared gold(I)-tetrahydrothiophene intermediate to yield gold(I) complexes

DOI: 10.1021/acs.inorgchem.8b03069
Inorg. Chem. 2019, 58, 2501−2513

2a–**2d** in near-quantitative yields. The stability of the gold(I)-phosphine complexes allows further reactions to take place without effecting the integrity of the complex. The second 4-(diphenylphosphosphino)benzoic acid was introduced to the gold complex using identical coupling conditions to those employed in the first synthetic step, resulting in cationic cyclic gold complexes **3a**–**3d**. The final step introduces the ruthenium(II) center via the coordination of one of the phosphine ligands previously interacting with the gold(I) center.

All compounds were characterized by ^{1}H, ^{31}P{^{1}H}, and ^{13}C{^{1}H} NMR spectroscopy, high-resolution mass spectrometry, and elemental analysis. The coordination of the ligands to the metal centers was monitored by ^{31}P{^{1}H} NMR spectroscopy. The phosphine ligand coordinated to the ruthenium center produces a characteristic singlet at ca. 25 ppm, whereas the gold-phosphine peak is observed at ca. 33 ppm (cf. ca. −5 ppm for the free ligand), allowing the reactions to be easily monitored. The introduction of a second 4-(diphenylphosphosphino)benzoic acid to **2a**–**2d** results in changes of differing magnitudes in the ^{31}P{^{1}H} NMR spectra, depending on the number of PEG units the complex possesses. The resulting cyclic gold(I) complexes **3a**–**3d** present a single broad peak at 29.53 (**3a**), 31.78 (**3b**), 28.20 (**3c**), and 31.09 (**3d**) ppm. The broad ^{31}P{^{1}H} NMR peaks observed for **3a**–**3d** can be attributed to the strain placed on the Au–P bonds by the cyclization, leading to fluctuations in the environment of the phosphorus. Upon the introduction of the ruthenium(II) center, **3a**–**3d** decyclize, and two peaks are observed in the ^{31}P{^{1}H} NMR spectra, as mentioned above at ca. 25 and 33 ppm for the ruthenium(II) and gold(II) coordinated phosphine ligands, respectively (Figure 2).

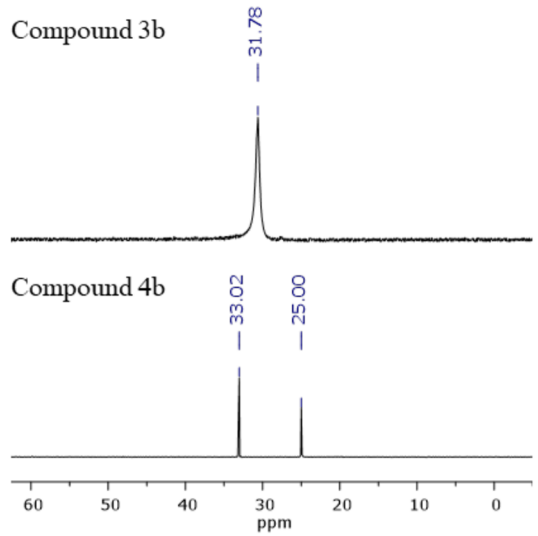

Figure 2. ^{31}P{^{1}H} NMR spectra (162 MHz, $CDCl_3$) of the cyclic gold complex **3b** (top) and heterobimetallic complex **4b** (bottom).

The ^{1}H NMR spectra of the target complexes **4a**–**4d** confirmed their formation with the appearance of the distinctive *p*-cymene peaks including doublets at 5.20–5.22 and 4.97–4.99 ppm, septet at 2.80–2.88 ppm, singlet at 1.85–1.86 ppm, and a doublet at 1.09–1.12 ppm. The coordination of a phosphine ligand to the ruthenium was observed via a downfield shift of the (*Ar*)C–CH–C*H*–C–P–Ru phenyl protons from 7.28 to 7.46 ppm (**3a**–**3d**) to 7.77–7.83 ppm (**4a**–**4d**) as well as the O–(C═O)–(*Ar*)C–C*H*–C*H*–C–P–Ru protons from 7.28 to 7.46 ppm (**3a**–**3d**) to 7.89–7.95 ppm (**4a**–**4d**) (Figure 3).

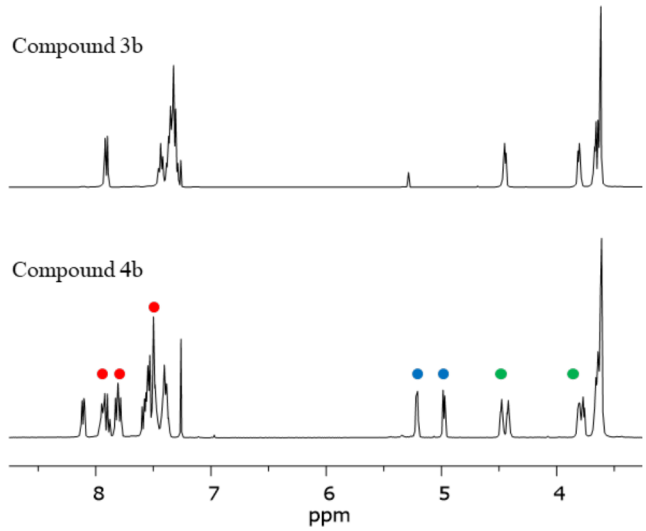

Figure 3. ^{1}H NMR (400 MHz, $CDCl_3$) spectra of cyclic gold complex **3b** (top) and heterobimetallic complex **4b** (bottom). Notable resonances are identified with colored circles: phenyl protons (red), η^6-arene protons (blue), and PEG protons (green).

***In Vitro* Antiproliferative Activity.** The antiproliferative activity of **4a**–**4d** was assessed using the 3-(4,5-dimethyl-2-thiazolyl)-2,5-diphenyl-2*H*-tetrazolium bromide (MTT) assay against cisplatin sensitive and resistant human ovarian carcinoma (A2780 and A2780cisR) and nontumoral human embryonic kidney (HEK-293) cell lines (Table 1).[43] Cisplatin, auranofin, and RAPTA-C were tested as controls.

Table 1. *In vitro* Antiproliferative Activity of 4a–4d, Cisplatin, Auranofin, and RAPTA-C against Human Ovarian Carcinoma (A2780), Human Ovarian Carcinoma Cisplatin Resistant (A2780cisR), and Human Embryonic Kidney 293 (HEK-293) Cell Lines after 72 h Exposure[a]

compound	A2780	A2780 CisR	HEK293
4a	2.5 ± 0.3	3.1 ± 0.3	2.7 ± 0.1
4b	2.4 ± 0.5	3.1 ± 0.1	2.7 ± 0.1
4c	2.4 ± 0.3	3.6 ± 0.4	2.9 ± 0.3
4d	1.8 ± 0.6	3.9 ± 0.5	3.5 ± 0.4
cisplatin	1.9 ± 0.4	13.3 ± 1.2	9 ± 0.8
auranofin[44]	1.3 ± 0.5	1.5 ± 0.5	1.9 ± 0.6
RAPTA-C	>200	>200	>200

[a]Values are given as the mean ± SD (μM).

The cytotoxicity of the parent complex, RAPTA-C, is low against a range of cell lines, with an IC_{50} > 200 μM against the tested cell lines. Compounds **4a**–**4d** possess IC_{50} values in the low micromolar range against all tested cell lines, with values comparable to those of cisplatin and auranofin against the A2780 cell line and to auranofin against the A2780 CisR cell line. Although the compounds overcome cisplatin resistance, they do not show selectivity toward the tumoral cell lines compared to the nontumoral cell lines. Moreover, the length of the PEG linker has negligible impact on the cytotoxicity of the complexes, showing that the cytotoxicity of these complexes is

DOI: 10.1021/acs.inorgchem.8b03069
Inorg. Chem. 2019, 58, 2501–2513

independent of linker length, as observed with homobimetallic ruthenium(II) and gold(I) complexes.[44]

Compounds **4a**–**4d** are considerably more cytotoxic toward the A2780 cell line compared to [(1-methyl-3-(4-((4′-methyl-2,2′-bipyridin-4-yl)methylcarbamoyl)benzyl)imidazole-2-ylidine gold(I) chloride][(η^6-*p*-cymene)ruthenium(II) chloride] hexafluorophosphate and [(1-methyl-3-(4-((4′-methyl-2,2′-bipyridin-4-yl)methylcarbamoyl)benzyl)imidazole-2-ylidine gold(I) (thiolato-β-D-glucose tetraacetate)][(η^6-*p*-cymene)-ruthenium(II) chloride] hexafluoro-phosphate, which possess IC_{50} values of 63.4 ± 2.4 and 16.8 ± 3.1 μM, respectively.[40] [(η^6-*p*-Cymene)$RuCl_2$(μ-dppm)Au(NHC)]ClO_4 (where NHC = N-heterocyclic carbene) complexes possess cytotoxicity greater than that of cisplatin against human renal (Caki-1) cells with IC_{50} values in the low micromolar range. They show good selectivity toward nontumoral HEK-293 cells compared to **4a**–**4d** with IC_{50} values of ≥73 μM.[42] The bimetallic compounds [(η^6-*p*-cymene)$RuCl_2$(μ-dppm)AuCl] (RUAU-1, Figure 1) and [(η^6-*p*-cymene)$RuCl_2$(μ-dppm)Au(S-thiazoline)] show comparable cytotoxicity toward human colon (HCT-116) cells to the Ru(*p*-cymene)Cl_2(μ-dppm)Au(NHC)]ClO_4 complexes with IC_{50} values of 4.6 ± 0.1 μM (1) and 6.5 ± 0.1 μM (2) versus 8–10 μM for the cationic NHC complexes.[41] RANCE-1 (Figure 1) also presents comparable cytotoxicity to the cationic NHC complexes with an IC_{50} of 8.7 ± 0.9 μM against Caki-1 cells, which is around threefold more cytotoxic than cisplatin but threefold less cytotoxic than auranofin against the same cell line.[39]

Amino Acid and Peptide Binding Studies. The ability of the heterobimetallic complexes to bind to the amino acid residues present in the RU1, RU2, AU1, and AU1′ binding sites in the nucleosome core particle was assessed using amino acids and a model peptide. In crystallographic studies on the nucleosome core particle, auranofin binds to histidine residues while RAPTA-T binds to both histidine and glutamine residues.[11] Complex **4b** was incubated with L-histidine for 2 h in a 1:1 complex–amino acid ratio in unbuffered solution (98% Milli-Q water, 2% DMSO) at 310 K, and the adducts were analyzed by mass spectrometry.[45−47] ESI-MS revealed a peak at *m*/*z* 894.6949 corresponding to the adduct [**4b** − 3Cl + 3His + 2K]$^{2+}$, in which dissociation of the three labile chloride ligands and subsequent binding of three histidine residues indicates that both the ruthenium and gold centers bind to histidines.

Peptide binding studies were performed on a fragment of the amyloid β-protein (residues 1–16, H-Asp^1-Ala^2-Glu^3–Phe^4-Arg^5-His^6-Asp^7-Ser^8-Gly^9-Tyr^{10}-Glu^{11}-Val^{12}-His^{13}-His^{14}-Gln^{15}-Lys^{16}–OH). Complex **4a** was incubated with the 16-*mer* for 2 h in a 1:3 complex–peptide ratio in unbuffered solution (98% Milli-Q, 2% DMSO) at 310 K. A 1:3 complex–peptide ratio was required to suppress the facile ionization of the gold center that suppresses the signal of peptide complex adducts. ESI-MS revealed 1:1 adducts of **4a** and the 1–16 amyloid β-peptide; 1:2 complex–peptides adducts were not observed (Figure 4). The loss of the three labile chloride ligands in the complex indicates that both the ruthenium and gold centers are coordinated to at least one amino acid residue cross-linking the peptide. Complex **4d**, possessing the longest linker of the series of PEG_8, was incubated with the 1–16 amyloid β-peptide under identical conditions. Similarly to **4a**, 1:1 complex–peptide adducts were observed, while 1:2 complex–peptide adducts were not found. To obtain further information on the mode of binding in the 1:1 adduct

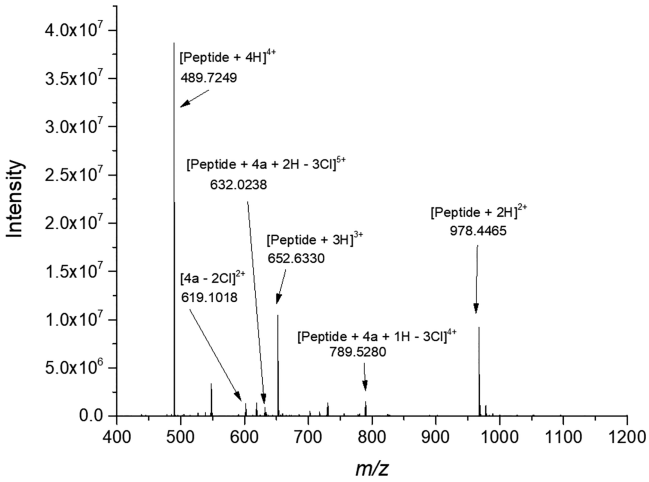

Figure 4. ESI-MS spectrum of **4a** incubated with 1–16 amyloid β-peptide in a 1:3 complex–peptide ratio at 310 K for 2 h (peaks of interest are labeled).

observed, the [peptide + **4a** + 2H − 3Cl]$^{5+}$ ion ($C_{140}H_{179}AuN_{27}O_{35}P_2Ru^{5+}$; theoretical *m*/*z* 631.8243; observed *m*/*z* 631.8235; −1.16 ppm) (Figure S21) was chosen for fragmentation due to its high charge state and intact **4a** adduct. Collision induced dissociation (CID), producing predominantly b- and y-type fragments,[48] and electron-transfer dissociation (ETD) fragmentation, which breaks N–C_α bonds along the peptide backbone producing c- and z-type fragments,[49] were performed. ETD fragmentation has recently been used to evaluate the binding of dinuclear ruthenium(II)-arene complexes on the amyloid β-peptide where the metal centers were found to bind to histidine residues.[50] The analysis of the fragments produced was performed using an online Apm^{2}s application (available on http://www.cheminfo.org/flavor/mass/index.html),[46,51] which enabled the identification of both terminal and internal fragments that are otherwise difficult to identify manually.

As both the ruthenium and gold centers can bind to histidine, it is likely that the [peptide + **4a** + 5H − 3Cl]$^{5+}$ ion represents a mixture of adducts in which the metals interact with His^6, His^{13}, and His^{14} in different combinations. The unmetalated peptide fragments produced by the CID and ETD fragmentation processes reveal an interesting pattern (Figure 5). The unmetalated CID fragments b_6–b_{15} and y_4–y_{15} were observed, whereas the smaller fragments, y_1–y_3 and b_1–b_5, were not present. The smallest fragments, b_6 and y_4, consist of residues H-Asp^1-Ala^2-Glu^3–Phe^4-Arg^5-His^6 and His^{13}-His^{14}-Gln^{15}-Lys^{16}–OH, respectively. In both directions, the fragmentation process is interrupted at a histidine residue, His^6 for b fragments and His^{13} for y fragments, suggesting that there is obstruction, presumably a bound metal center, which interrupts fragmentation. The ETD fragmentation reveals an identical pattern where the unmetalated peptide fragments, c_6, c_7, c_9–c_{13}, c_{15}, and z_4–z_{14} fragments, were observed (Figure 5). The smallest fragments observed, c_6 and z_4, also consist of H-Asp^1-Ala^2-Glu^3-Phe^4-Arg^5-His^6 and His^{13}-His^{14}-Gln^{15}-Lys^{16}–OH, respectively. The similarity between the CID and ETD fragmentation patterns suggest that the obstruction occurs at His^6 and His^{13}, impeding both fragmentation processes.

Interestingly, the series of ETD peptide fragments containing bound **4a** (Figure 6) mirror the unmetalated ETD fragments (Figure 5). The fragments c_6*–c_{15}* and z_5*–

DOI: 10.1021/acs.inorgchem.8b03069
Inorg. Chem. 2019, 58, 2501−2513

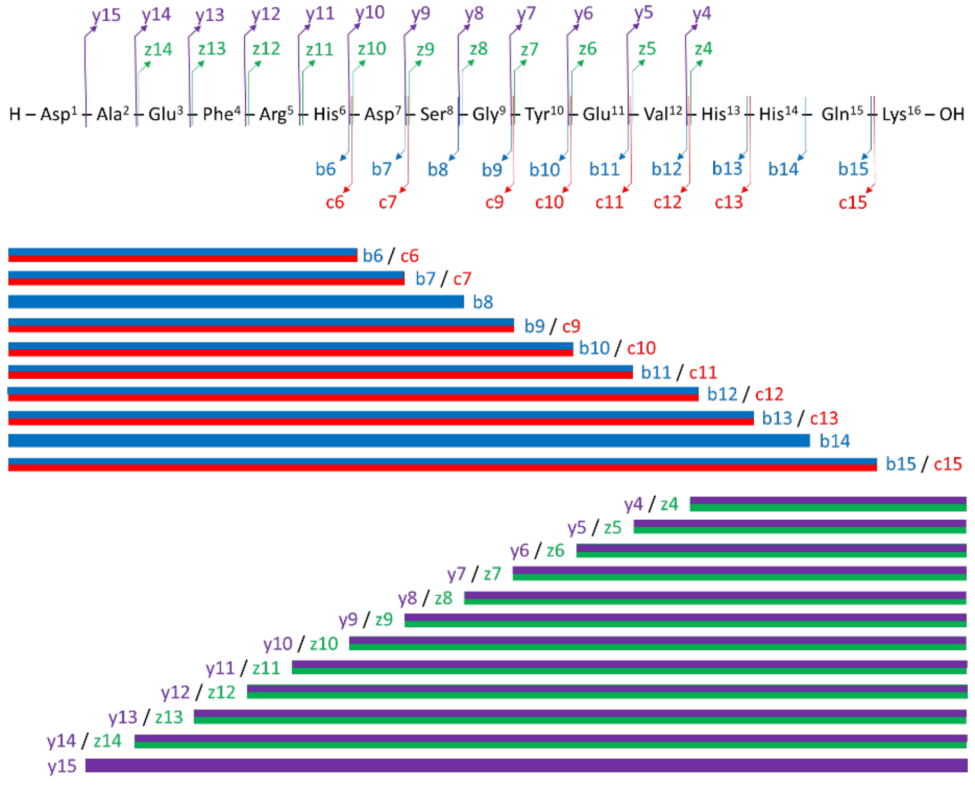

Figure 5. Fragmentation of the [peptide + **4a** + 2H − 3Cl]$^{5+}$ ion (m/z 631.8235): unmetalated CID, b (blue) and y (purple), and ETD, c (red) and z (green), fragments.

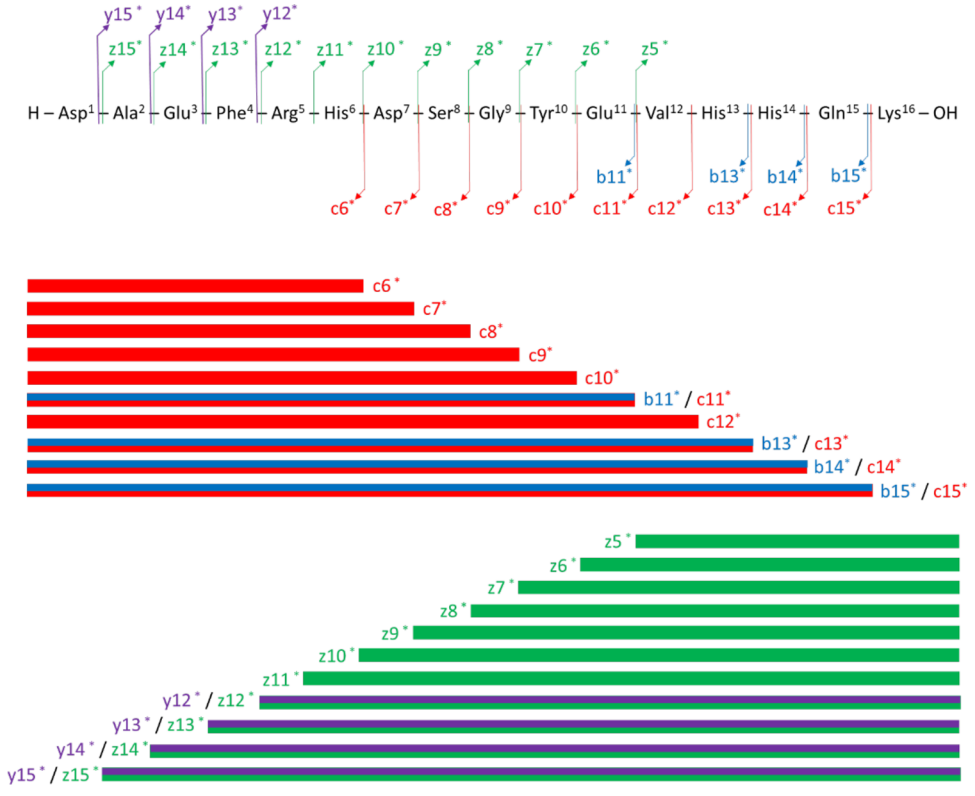

Figure 6. Fragmentation of the [peptide + **4a** + 2H − 3Cl]$^{5+}$ ion (m/z 631.8235): metalated CID, b (blue) and y (purple), and ETD, c (red) and z (green), fragments containing the [**4a** − 3Cl] adduct.

z_{15}* containing the complete [**4a** − 3Cl] adduct are observed. The smallest fragments, c_6 and z_5, consisting of H-Asp^1-Ala^2-Glu^3-Phe^4-Arg^5-His^6 and His^{13}-His^{14}-Gln^{15}-Lys^{16}−OH residues, respectively, are identical to the nonmetalated fragments.

DOI: 10.1021/acs.inorgchem.8b03069
Inorg. Chem. 2019, 58, 2501−2513

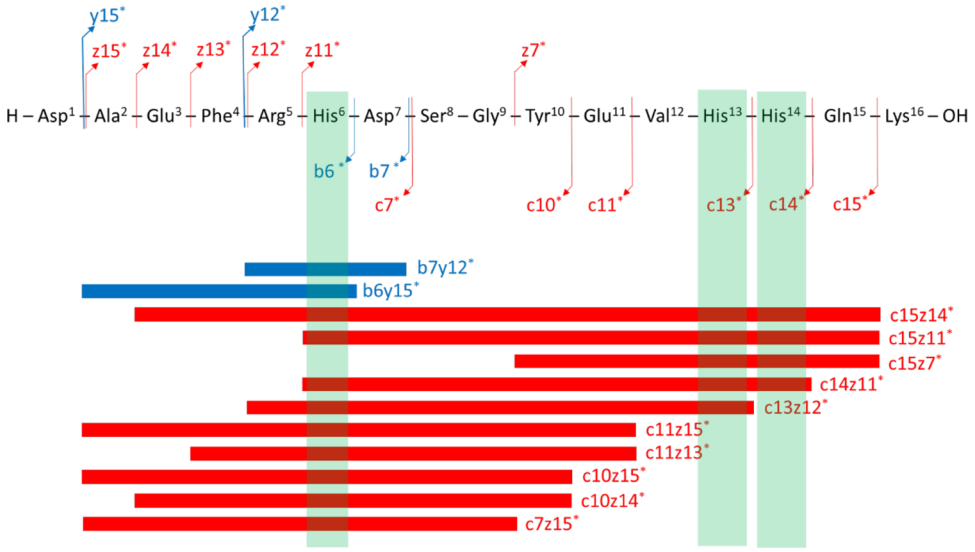

Figure 7. Fragmentation of the [peptide + **4a** + 2H − 3Cl]$^{5+}$ ion (m/z 631.8235): metalated CID, b_xy_x (blue), and ETD, c_xz_x (red), internal fragments containing the [**4a** − 3Cl] adduct.

As it is plausible that both the gold and the ruthenium centers could bind to any of the His^6, His^{13}, and His^{14} sites, a ruthenium or gold center bound to the His^6 and His^{13} residues could be impeding further fragmentation of the peptide-**4a** adduct. Metalated b- and y-type fragments containing [**4a** − 3Cl] are also observed in the CID spectrum (Figure 6); however, the smallest fragments found are b_{11}* and y_{12}* and do not yield much information.

However, the observed unmetalated internal fragments only include one, if any, histidine residues. Fragments $c_{13}z_8$, $c_{13}z_7$ and $c_{13}z_6$ include the His^{13} residue and the c_7z_{13}, c_7z_{14}, c_7z_{15}, c_9z_{12}, c_9z_{14}, $c_{10}z_{15}$ and fragments include the His^6 residue. The other unmetalated fragments observed internal fragments, c_4z_{15} and $c_{12}z_9$, do not contain any histidines residues. This suggests that the histidine residues that are not included in the fragments could be bound to **4a**.

In contrast, all the observed metalated CID and ETD internal fragments containing the [**4a** −3Cl] adducts contain at least one histidine residue (Figure 7). The CID internal fragments b_6y_{15}* and b_7y_{12}*, contain Ala^2-Glu^3-Phe^4-Arg^5-His^6 and Arg^5-His^6-Asp^7 residues, indicating that either the gold or ruthenium centers are bound to the His^6 residue. On the other hand, the metalated internal ETD fragments include all three histidine residues in different combinations. Fragments $c_{11}z_{15}$*, $c_{11}z_{13}$*, $c_{10}z_{15}$*, $c_{10}z_{14}$*, and c_7z_{15}* contain the His^6 residue; $c_{13}z_{12}$* contains the His^{13}, and $c_{15}z_7$* contains both His^{13} and His^{14}. Fragments $c_{15}z_{14}$*, $c_{15}z_{11}$*, and $c_{14}z_{11}$* contain all three histidine residues His^6, His^{13}, and His^{14}, suggesting that the gold and ruthenium centers are both bound to the fragment via at least one histidine.

Concluding Remarks. A series of heterometallic ruthenium(II)−gold(I) complexes inspired by the preferential binding of RAPTA-T and auranofin in the nucleosome core particle was synthesized with different lengths of linkers ranging from 4 to 8 PEG units. They possess cytotoxicities in the low micromolar range against A2780, A2780cisR, and HEK293 cell lines. Although they do not show selectivity toward cancer cells, they do have the ability to overcome cisplatin resistance in the A2780cisR cell line. Binding studies performed on L-histidine and the 1−16 *mer* amyloid β-protein show that the both the ruthenium and gold centers can bind to histidine residues, suggesting that these complexes have the capability to bind to the RU2, AU1, and AU1′ binding sites on the nucleosome core particle.

EXPERIMENTAL SECTION

Materials. All commercially available starting materials were purchased from Sigma-Aldrich, TCI, ABCR and used without further purification. Ruthenium trichloride hydrate was purchased from precious metals online and used in the synthesis of the [Ru(*p*-cymene)Cl$_2$]$_2$ dimer.[52] L-histidine was purchased from ABCR and the 1−16 β-amyloid peptide (H-Asp-Ala-Glu-Phe-Arg-His-Asp-Ser-Gly-Tyr-Glu-Val-His-His-Gln-Lys−OH) was purchased as a trifluoroacetate salt from Bachem. Dichloromethane was purified and degassed using a PureSolv solvent purification system (Innovative Technology INC) prior to use. Reactions were monitored via thin-layer chromatography carried out on silica plates (Merck 5554) and visualized under UV radiation (254 nm). Flash column chromatography was conducted in the normal phase on a CombiFlash-EZ prep machine installed with prepacked Luknova columns and the stated eluent system.

Instrumentation and Methods. ^{1}H (400 MHz), ^{31}P{^{1}H} (101 MHz), and ^{13}C{^{1}H} (162 MHz) NMR spectra were conducted on a Bruker Advance II 400 and referenced to the residual solvent peak of $CDCl_3$ (^{1}H: 7.26 ppm, ^{13}C: 77.16 ppm). Coupling constants (J) are reported in hertz. High-resolution ESI-MS characterization was performed on a Xevo G2-S QTOF mass spectrometer coupled to the Acquity UPLC Class Binary Solvent manager and BTN sample manager (Waters, Corporation, Milford, MA). Elemental Analysis was performed on a Thermo Scientific Flash 2000 organic elemental analyzer.

Synthesis. *General Procedure of **1a**−**1d**.* 4-(Diphenylphosphino)benzoic acid (1 equiv) and EDCI (1.3 equiv) were dissolved in dry CH_2Cl_2 (3 mL) and stirred under N_2 at room temperature for 1 h. The solution was added dropwise to a solution of the appropriate ethylene glycol (1.5 equiv) and DMAP (0.5 equiv) in dry CH_2Cl_2 (2 mL), and the reaction was stirred under N_2 at room temperature for 21 h. The reaction mixture was washed with brine (100 mL), dried over anhydrous sodium sulfate, filtered and concentrated under reduced pressure. Purification was achieved via flash column chromatography using an eluent system of C_6H_{14}/EtOAc and the product was isolated as a colorless oil.

*Compound **1a**.* According to the general procedure, 4-(diphenylphosphino)benzoic acid (0.300 g, 0.979 mmol, 1 equiv), EDCI (0.244 g, 1.273 mmol, 1.3 equiv), tetraethylene glycol (0.285 g,

DOI: 10.1021/acs.inorgchem.8b03069
Inorg. Chem. 2019, 58, 2501−2513

1.273 mmol,0.25 mL, 1.5 equiv), and DMAP (0.060 g, 0.490 mmol, 0.5 equiv) in CH_2Cl_2 (5 mL). The product was isolated as a colorless oil (0.291 g, 0.603 mmol, 62%); Elemental Analysis (%): calcd for $C_{27}H_{31}O_6P$ C 67.21 H 6.48; found C 67.20 H 6.42. ^1H NMR ($CDCl_3$, 400 MHz): 7.97−8.00 (2H, m, 2×O−(C═O)−(*Ar*)C−C*H*−CH−C−P), 7.26−7.38 (12H, m, 2×O−(C═O)−(*Ar*)C−CH−C*H*−C−P, 4×P−(*Ar*)C−C*H*−CH−CH, 4×P−(*Ar*)C−CH−C*H*−CH, 2×P−(*Ar*)C−CH−CH−C*H*), 4.46−4.49 (2H, m, *Ar*−(C═O)−O−C*H*$_2$−CH$_2$−O), 3.80−3.83 (2H, m, *Ar*−(C═O)−O−CH$_2$−C*H*$_2$−O), 3.60−3.71 (10H, m, *Ar*−(C═O)−O−(CH$_2$)$_2$−O−(C*H*$_2$)$_2$, *Ar*−(C═O)−O−((CH$_2$)$_2$−O)$_2$−(C*H*$_2$)$_2$, *Ar*−(C═O)−O−((CH$_2$)$_2$−O)$_3$−CH$_2$−C*H*$_2$−OH), 3.57−3.60 (2H, m, *Ar*−(C═O)−O−((CH$_2$)$_2$−O)$_3$−CH$_2$−C*H*$_2$−OH); ^{31}P {^1H} NMR ($CDCl_3$, 162 MHz): −4.95 (1P); ^{13}C {^1H} NMR ($CDCl_3$, 101 MHz): 166.4 (1C, O−(*C*═O)−(*Ar*)C−CH−CH−C−P), 144.3 (1C, d, O−(C═O)−(*Ar*)C−CH−CH−*C*−P, $^1J_{C,P}$ = 14 Hz), 136.3 (2C, d, 2×P−(*Ar*)*C*−CH−CH−CH, $^1J_{C,P}$ = 11 Hz), 134.1 (4C, d, 4×P−(*Ar*)C−*C*H−CH−CH, $^2J_{C,P}$ = 20 Hz), 133.3 (2C, d, 2×O−(C═O)−(*Ar*)C−CH−*C*H−C−P, $^2J_{C,P}$ = 19 Hz), 130.1 (1C, O−(C═O)−(*Ar*)*C*−CH−CH−C−P), 129.5 (2C, d, 2×O−(C═O)−(Ar)C−*C*H−CH−C−P, $^3J_{C,P}$ = 6 Hz), 129.2 (2C, 2×P−(*Ar*)C−CH−CH−*C*H), 128.8 (4C, d, 4×P−(*Ar*)C−CH−*C*H−CH, $^3J_{C,P}$ = 7 Hz), 72.6 (1C, O−*C*H$_2$−CH$_2$−OH), 70.8 (2C, *Ar*−(C═O)−O−((CH$_2$)$_2$−O)$_2$-*C*H$_2$, *Ar*−(C═O)−O−(CH$_2$)$_2$−O−CH$_2$-*C*H$_2$), 70.7 (1C, *Ar*−(C═O)−O−((CH$_2$)$_2$−O)$_2$−CH$_2$−*C*H$_2$), 70.5 (1C, *Ar*−(C═O)−O−(CH$_2$)$_2$−O−*C*H$_2$), 69.3 (1C, (*Ar*)−(C═O)−O−CH$_2$−*C*H$_2$−O), 64.2 (1C, (*Ar*)−(C═O)−O−*C*H$_2$−CH$_2$−O), 61.9 (1C, O−CH$_2$−*C*H$_2$−OH), 2.19 (1H, bs, −O*H*); HRMS (ESI(+)-QTOF): *m*/*z* found 483.1938 $[M + H]^+$ $C_{27}H_{32}O_6P^+$ requires 483.1931 (ppm = 1.45), 505.1768 $[M + Na]^+$ $C_{27}H_{31}O_6PNa$ requires 505.1750 (ppm = 3.56).

Compound ***1b***. According to the general procedure, 4-(diphenylphosphino)benzoic acid (0.300 g, 0.979 mmol, 1 equiv), EDCI (0.244 g, 1.273 mmol, 1.3 equiv), pentaethylene glycol (0.350 g, 1.469 mmol, 0.31 mL, 1.5 equiv), and DMAP (0.060 g, 0.490 mmol, 0.5 equiv) in CH_2Cl_2 (5 mL). The product was isolated as a colorless oil (0.340 g, 0.646 mmol, 66%); Elemental Analysis (%): calcd For $C_{29}H_{35}O_7P$ C 66.15 H 6.70; found C 66.02 H 6.66; ^1H NMR ($CDCl_3$, 400 MHz): 7.97−8.00 (2H, m, 2×O−(C═O)−(*Ar*)C−C*H*−CH−C−P), 7.26−7.38 (12H, m, 2×O−(C═O)−(*Ar*)C−CH−C*H*−C−P, 4×P−(*Ar*)C−C*H*−CH−CH, 4×P−(*Ar*)C−CH−C*H*−CH, 2×P−(*Ar*)C−CH−CH−C*H*), 4.45−4.48 (2H, m, *Ar*−(C═O)−O−C*H*$_2$−CH$_2$−O), 3.80−3.83 (2H, m, *Ar*−(C═O)−O−CH$_2$−C*H*$_2$−O), 3.60−3.71 (16H, m, *Ar*−(C═O)−O−(CH$_2$)$_2$−O−(C*H*$_2$)$_2$, *Ar*−(C═O)−O−((CH$_2$)$_2$−O)$_2$−(C*H*$_2$)$_2$, *Ar*−(C═O)−O−((CH$_2$)$_2$−O)$_3$−(C*H*$_2$)$_2$, *Ar*−(C═O)−O−((CH$_2$)$_2$−O)$_4$−(C*H*$_2$)$_2$−OH, 2.19 (1H, bs, −O*H*); ^{31}P {^1H} NMR ($CDCl_3$, 162 MHz): −5.05 (1P); ^{13}C {^1H} NMR ($CDCl_3$, 101 MHz): 166.5 (1C, O−(*C*═O)−(*Ar*)C−CH−CH−C−P), 144.3 (1C, d, O−(C═O)−(*Ar*)C−CH−CH−*C*−P, $^1J_{C,P}$ = 14 Hz), 136.3 (2C, d, 2×P−(*Ar*)*C*−CH−CH−CH, $^1J_{C,P}$ = 11 Hz), 134.1 (4C, d, 4×P−(*Ar*)C−*C*H−CH−CH, $^2J_{C,P}$ = 20 Hz), 133.3 (2C, d, 2×O−(C═O)−(*Ar*)C−CH−*C*H−C−P, $^2J_{C,P}$ = 19 Hz), 130.2 (1C, O−(C═O)−(*Ar*)*C*−CH−CH−C−P), 129.5 (2C, d, 2×O−(C═O)−(Ar)C−*C*H−CH−C−P, $^3J_{C,P}$ = 6 Hz), 129.3 (2C, 2×P−(*Ar*)C−CH−CH−*C*H), 128.8 (4C, d, 4×P−(*Ar*)C−CH−*C*H−CH, $^3J_{C,P}$ = 7 Hz), 72.6 (1C, O−*C*H$_2$−CH$_2$−OH), 70.7−70.8 (5C, *Ar*−(C═O)−O−(CH$_2$)$_2$−O−CH$_2$− *C*H$_2$, *Ar*−(C═O)−O−((CH$_2$)$_2$−O)$_2$−(*C*H$_2$)$_2$, *Ar*−(C═O)−O−((CH$_2$)$_2$−O)$_3$−(*C*H$_2$)$_2$), 70.5 (1C, *Ar*−(C═O)−O−(CH$_2$)$_2$−O−*C*H$_2$), 69.3 (1C, (*Ar*)−(C═O)−O−CH$_2$−*C*H$_2$−O), 64.2 (1C, (*Ar*)−(C═O)−O−*C*H$_2$−CH$_2$−O), 61.9 (1C, O−CH$_2$−*C*H$_2$−OH); HRMS (ESI(+)-QTOF): *m*/*z* found 527.2198 $[M + H]^+$ $C_{29}H_{36}O_7P^+$ requires 527.2193 (ppm = 0.95), 549.2040 $[M + Na]^+$ $C_{29}H_{35}O_7PNa$ requires 549.2013 (ppm = 4.92).

Compound ***1c***. According to the general procedure, 4-(diphenylphosphino)benzoic acid (0.300 g, 0.979 mmol, 1 equiv), EDCI (0.244 g, 1.273 mmol, 1.3 equiv), hexaethylene glycol (0.414 g, 1.469 mmol, 0.37 mL, 1.5 equiv), and DMAP (0.060 g, 0.490 mmol, 0.5 equiv) in CH_2Cl_2 (5 mL). The product was isolated as a colorless oil (0.372 g, 0.652 mmol, 67%); Elemental Analysis (%): calcd for $C_{31}H_{39}O_8P$ C 65.25 H 6.89; found C 65.16 H 6.93; ^1H NMR ($CDCl_3$, 400 MHz): 7.97−7.99 (2H, m, 2×O−(C═O)−(*Ar*)C−C*H*−CH−C−P), 7.29−7.38 (12H, m, 2×O−(C═O)−(*Ar*)C−CH−C*H*−C−P, 4×P−(*Ar*)C−C*H*−CH−CH, 4×P−(*Ar*)C−CH−C*H*−CH, 2×P−(*Ar*)C−CH−CH−C*H*), 4.45−4.47 (2H, m, *Ar*−(C═O)−O−C*H*$_2$−CH$_2$−O), 3.80−3.83 (2H, m, *Ar*−(C═O)−O−CH$_2$−C*H*$_2$−O), 3.58−3.72 (20H, m, *Ar*−(C═O)−O−(CH$_2$)$_2$−O−(C*H*$_2$)$_2$, *Ar*−(C═O)−O−((CH$_2$)$_2$−O)$_2$−(C*H*$_2$)$_2$, *Ar*−(C═O)−O−((CH$_2$)$_2$−O)$_3$−(C*H*$_2$)$_2$, *Ar*−(C═O)−O−((CH$_2$)$_2$−O)$_5$−(C*H*$_2$)$_2$, *Ar*−(C═O)−O−((CH$_2$)$_2$−O)$_5$−(C*H*$_2$)$_2$−OH, 2.65 (1H, bs, −O*H*); ^{31}P {^1H} NMR ($CDCl_3$, 162 MHz): −4.84 (1P); ^{13}C {^1H} NMR ($CDCl_3$, 101 MHz): 166.4 (1C, O−(*C*═O)−(*Ar*)C−CH−CH−C−P), 144.3 (1C, d, O−(C═O)−(*Ar*)C−CH−CH−*C*−P, $^1J_{C,P}$ = 14 Hz), 136.3 (2C, d, 2×P−(*Ar*)*C*−CH−CH−CH, $^1J_{C,P}$ = 11 Hz), 134.1 (4C, d, 4×P−(*Ar*)C−*C*H−CH−CH, $^2J_{C,P}$ = 20 Hz), 133.3 (2C, d, 2×O−(C═O)−(*Ar*)C−CH−*C*H−C−P, $^2J_{C,P}$ = 19 Hz), 130.2 (1C, O−(C═O)−(*Ar*)*C*−CH−CH−C−P), 129.5 (2C, d, 2×O−(C═O)−(Ar)C−*C*H−CH−C−P, $^3J_{C,P}$ = 6 Hz), 129.3 (2C, 2×P−(*Ar*)C−CH−CH−*C*H), 128.8 (4C, d, 4×P−(*Ar*)C−CH−*C*H−CH, $^3J_{C,P}$ = 7 Hz), 72.7 (1C, O−*C*H$_2$−CH$_2$−OH), 70.7−70.8 (7C, *Ar*−(C═O)−O−(CH$_2$)$_2$−O−CH$_2$-*C*H$_2$, *Ar*−(C═O)−O−((CH$_2$)$_2$−O)$_2$−(*C*H$_2$)$_2$, *Ar*−(C═O)−O−((CH$_2$)$_2$−O)$_3$−(*C*H$_2$)$_2$, *Ar*−(C═O)−O−((CH$_2$)$_4$−O)$_2$−(*C*H$_2$)$_2$), 70.5 (1C, *Ar*−(C═O)−O−(CH$_2$)$_2$−O−*C*H$_2$), 69.3 (1C, (*Ar*)−(C═O)−O−CH$_2$−*C*H$_2$−O), 64.3 (1C, (*Ar*)−(C═O)−O−*C*H$_2$−CH$_2$−O), 61.9 (1C, O−CH$_2$−*C*H$_2$−OH); HRMS (ESI(+)-QTOF): *m*/*z* found 571.2467 $[M + H]^+$ $C_{31}H_{40}O_8P^+$ requires 571.2461 (ppm = 1.05).

Compound ***1d***. According to the general procedure, 4-(diphenylphosphino)benzoic acid (0.300 g, 0.979 mmol, 1 equiv), EDCI (0.244 g, 1.273 mmol, 1.3 equiv), octaethylene glycol (0.544 g, 1.469 mmol, 1.5 equiv), and DMAP (0.060 g, 0.490 mmol, 0.5 equiv) in CH_2Cl_2 (5 mL). The product was isolated as a colorless oil (0.309 g, 0.469 mmol, 48%); Elemental Analysis (%): calcd for $C_{35}H_{47}O_{10}P\cdot C_6H_{14}$ C 66.11 H 8.25, found C 66.31 H 8.02; ^1H NMR ($CDCl_3$, 400 MHz): 7.96−7.98 (2H, m, 2×O−(C═O)−(*Ar*)C−C*H*−CH−C−P), 7.30−7.36 (12H, m, 2×O−(C═O)−(*Ar*)C−CH−C*H*−C−P, 4×P−(*Ar*)C−C*H*−CH−CH, 4×P−(*Ar*)C−CH−C*H*−CH, 2×P−(*Ar*)C−CH−CH−C*H*), 4.44−4.46 (2H, m, *Ar*−(C═O)−O−C*H*$_2$−CH$_2$−O), 3.79−3.82 (2H, m, *Ar*−(C═O)−O−CH$_2$−C*H*$_2$−O), 3.58−3.72 (28H, m, *Ar*−(C═O)−O−(CH$_2$)$_2$−O−(C*H*$_2$)$_2$, *Ar*−(C═O)−O−((CH$_2$)$_2$−O)$_2$−O−(C*H*$_2$)$_2$, *Ar*−(C═O)−O−((CH$_2$)$_2$−O)$_3$−(C*H*$_2$)$_2$, *Ar*−(C═O)−O−((CH$_2$)$_2$−O)$_4$−(C*H*$_2$)$_2$, *Ar*−(C═O)−O−((CH$_2$)$_2$−O)$_5$−(C*H*$_2$)$_2$, *Ar*−(C═O)−O−((CH$_2$)$_2$−O)$_6$−(C*H*$_2$)$_2$, *Ar*−(C═O)−O−((CH$_2$)$_2$−O)$_7$−(C*H*$_2$)$_2$−OH); ^{31}P {^1H} NMR ($CDCl_3$, 162 MHz): −5.08 (1P); ^{13}C {^1H} NMR ($CDCl_3$, 101 MHz): 166.4 (1C, O−(*C*═O)−(*Ar*)C−CH−CH−C−P), 143.2 (1C, d, O−(C═O)−(*Ar*)C−CH−CH−*C*−P, $^1J_{C,P}$ = 14 Hz), 135.2 (2C, d, 2×P−(*Ar*)*C*−CH−CH−CH, $^1J_{C,P}$ = 11 Hz), 133.0 (4C, d, 4×P−(*Ar*)C−*C*H−CH−CH, $^2J_{C,P}$ = 20 Hz), 132.2 (2C, d, 2×O−(C═O)−(*Ar*)C−CH−*C*H−C−P, $^2J_{C,P}$ = 19 Hz), 129.1 (1C, O−(C═O)−(*Ar*)*C*−CH−CH−C−P), 128.5 (2C, d, 2×O−(C═O)−(Ar)C−*C*H−CH−C−P, $^3J_{C,P}$ = 6 Hz), 128.2 (2C, 2×P−(*Ar*)C−CH−CH−*C*H), 127.4 (4C, d, 4×P−(*Ar*)C−CH−*C*H−CH, $^3J_{C,P}$ = 7 Hz), 71.6 (1C, O−*C*H$_2$−CH$_2$−OH), 69.41−69.77 (12C, *Ar*−(C═O)−O−(CH$_2$)$_2$−O−(*C*H$_2$)$_2$, *Ar*−(C═O)−O−((CH$_2$)$_2$−O)$_2$−O−(*C*H$_2$)$_2$, *Ar*−(C═O)−O−((CH$_2$)$_2$−O)$_3$−(*C*H$_2$)$_2$, *Ar*−(C═O)−O−((CH$_2$)$_2$−O)$_4$−(*C*H$_2$)$_2$, *Ar*−(C═O)−O−((CH$_2$)$_2$−O)$_5$−(*C*H$_2$)$_2$, *Ar*−(C═O)−O−((CH$_2$)$_6$−O)$_2$−(*C*H$_2$)$_2$), 68.3 (1C, (*Ar*)−(C═O)−O−CH$_2$−*C*H$_2$−O), 63.3 (1C, (*Ar*)−(C═O)−O−*C*H$_2$−CH$_2$−O), 60.8 (1C, CH$_2$−*C*H$_2$−OH); HRMS (ESI(+)-QTOF): *m*/*z* found 681.2808 $[M + Na]^+$ $C_{35}H_{47}O_{10}PNa^+$ requires 681.2805 (ppm = 0.44).

General Procedure of ***2a−2d***. The appropriate monophosphine ligand (1 equiv) and freshly prepared AuCl(tht)[53] (1 equiv) were dissolved in CH_2Cl_2 (10 mL) and stirred under N_2 and rt for 18 h. The reaction mixture was concentrated to 1 mL under reduced pressure and was purified via flash column chromatography using

DOI: 10.1021/acs.inorgchem.8b03069
Inorg. Chem. 2019, 58, 2501−2513

CH_2Cl_2/CH_3OH as eluent. The product was isolated as a colorless oil.

Compound ***2a***. According to the general procedure, **1a** (0.291 g, 0.603 mmol, 1 equiv) and AuCl(tht) (0.193 g, 0.603 mmol, 1 equiv) in CH_2Cl_2 (10 mL). The product was isolated as a colorless oil (0.419 g, 0.587 mmol, 97%); Elemental Analysis (%): calcd for $C_{27}H_{31}AuClO_9P$ C 45.36 H 4.37; found C 45.71 H 4.57; ^{1}H NMR ($CDCl_3$, 400 MHz): 8.02−8.04 (2H, m, 2×O−(C═O)−(*Ar*)C−C*H*−CH−C−P), 7.38−7.51 (12H, m, 2×O−(C═O)−(*Ar*)C−CH−C*H*−C−P, 4×P−(*Ar*)C−C*H*−CH−CH, 4×P−(*Ar*)C−CH−C*H*−CH, 2×P−(*Ar*)C−CH−CH−C*H*), 4.38−4.40 (2H m, *Ar*−(C═O)−O−CH_2−CH_2−O), 3.72−3.74 (2H, m, *Ar*−(C═O)−O−CH_2−CH_2−O), 3.54−3.59 (10H, m, *Ar*−(C═O)−O−$(CH_2)_2$−O−(CH_2)$_2$, *Ar*−(C═O)−O−$((CH_2)_2$−O$)_2$−(CH_2)$_2$, *Ar*−(C═O)−O−$((CH_2)_2$−O$)_3$-CH_2), 3.45−3.47 (2H, m, O−CH_2−CH_2−OH); ^{31}P {^{1}H} NMR ($CDCl_3$, 162 MHz): 32.89 (1P); ^{13}C {^{1}H} NMR ($CDCl_3$, 101 MHz): 165.1 (1C, O−(C═O)−(*Ar*)C−CH−CH−C−P), 134.0 (1C, d, O−(C═O)−(*Ar*)C−CH−CH−C−P, $^1J_{C,P}$ = 60 Hz), 133.9 (4C, d, 4×P−(*Ar*)C−CH−CH−CH, $^2J_{C,P}$ = 14 Hz), 133.7 (2C, d, 2×O−(C═O)−(*Ar*)C−CH−CH−C−P, $^2J_{C,P}$ = 14 Hz), 133.0 (1C, O−(C═O)−(*Ar*)C−CH−CH−C−P, $^4J_{C,P}$ = 3 Hz), 132.2 (2C, 2×P−(*Ar*)C−CH−CH−CH, $^4J_{C,P}$ = 3 Hz), 129.9 (2C, d, 2×O−(C═O)−(Ar)C−CH−CH−C−P, $^3J_{C,P}$ = 12 Hz), 129.3 (4C, 4×P−(*Ar*)C−CH−CH−CH, $^3J_{C,P}$ = 12 Hz), 127.5 (2C, d, 2×P−(*Ar*)C−CH−CH−CH, $^1J_{C,P}$ = 63 Hz), 72.3 (1C, O−CH_2−CH_2−OH), 70.2−70.4 (3C, *Ar*−(C═O)−O−$(CH_2)_2$−O−CH_2-CH_2, *Ar*−(C═O)−O−$((CH_2)_2$−O$)_2$−(CH_2)$_2$), 70.0 (1C, *Ar*−(C═O)−O−$(CH_2)_2$−O−CH_2), 68.8 (1C, *Ar*−(C═O)−O−CH_2−CH_2), 64.4 (1C, *Ar*−(C═O)−O−CH_2−CH_2), 61.3 (1C, O−CH_2−CH_2−OH); HRMS (ESI(+)-QTOF): *m*/*z* found 737.1116 $[M + Na]^+$ $C_{27}H_{31}AuClO_6PNa^+$ requires 737.1110 (ppm = 0.81).

Compound ***2b***. According to the general procedure, **1b** (0.340 g, 0.646 mmol, 1 equiv) and AuCl(tht) (0.207 g, 0.646 mmol, 1 equiv) in CH_2Cl_2 (10 mL). The product was isolated as a colorless oil (0.482 g, 0.634 mmol, 98%); Elemental Analysis (%): calcd for $C_{29}H_{35}AuClO_7P$ C 45.89 H 4.65; found C 45.49 H 4.63; ^{1}H NMR ($CDCl_3$, 400 MHz): 8.08−8.11 (2H, m, 2×O−(C═O)−(*Ar*)C−C*H*−CH−C−P), 7.46−7.58 (12H, m, 2×O−(C═O)−(*Ar*)C−CH−C*H*−C−P, 4×P−(*Ar*)C−C*H*−CH−CH, 4×P−(*Ar*)C−CH−C*H*−CH, 2×P−(*Ar*)C−CH−CH−C*H*), 4.45−4.48 (2H m, *Ar*−(C═O)−O−CH_2−CH_2−O), 3.79−3.81 (2H, m, *Ar*−(C═O)−O−CH_2−CH_2−O), 3.58−3.68 (14H, m, *Ar*−(C═O)−O−$(CH_2)_2$−O−(CH_2)$_2$, *Ar*−(C═O)−O−$((CH_2)_2$−O$)_2$−(CH_2)$_2$, *Ar*−(C═O)−O−$((CH_2)_2$−O$)_3$−(CH_2)$_2$, *Ar*−(C═O)−O−$((CH_2)_2$−O$)_4$-CH_2), 3.54−3.57 (2H, m, O−CH_2−CH_2−OH); ^{31}P {^{1}H} NMR ($CDCl_3$, 162 MHz): 33.00 (1P); ^{13}C {^{1}H} NMR ($CDCl_3$, 101 MHz): 165.3 (1C, O−(C═O)−(*Ar*)C−CH−CH−C−P), 134.3 (1C, d, O−(C═O)−(*Ar*)C−CH−CH−C−P, $^1J_{C,P}$ = 60 Hz), 134.2 (4C, d, 4×P−(*Ar*)C−CH−CH−CH, $^2J_{C,P}$ = 14 Hz), 133.9 (2C, d, 2×O−(C═O)−(*Ar*)C−CH−CH−C−P, $^2J_{C,P}$ = 14 Hz), 133.3 (1C, O−(C═O)−(*Ar*)C−CH−CH−C−P, $^4J_{C,P}$ = 3 Hz), 132.4 (2C, 2×P−(*Ar*)C−CH−CH−CH, $^4J_{C,P}$ = 3 Hz), 130.2 (2C, d, 2×O−(C═O)−(Ar)C−CH−CH−C−P, $^3J_{C,P}$ = 12 Hz), 129.3 (4C, 4×P−(*Ar*)C−CH−CH−CH, $^3J_{C,P}$ = 12 Hz), 127.9 (2C, d, 2×P−(*Ar*)C−CH−CH−CH, $^1J_{C,P}$ = 63 Hz), 72.5 (1C, O−CH_2−CH_2−OH), 70.5−70.7 (5C, *Ar*−(C═O)−O−$(CH_2)_2$−O−CH_2-CH_2, *Ar*−(C═O)−O−$((CH_2)_2$−O$)_2$−(CH_2)$_2$, *Ar*−(C═O)−O−$((CH_2)_2$−O$)_3$−(CH_2)$_2$), 70.3 (1C, *Ar*−(C═O)−O−$(CH_2)_2$−O−CH_2), 69.1 (1C, *Ar*−(C═O)−O−CH_2−CH_2), 64.7 (1C, *Ar*−(C═O)−O−CH_2−CH_2), 61.7 (1C, O−CH_2−CH_2−OH); HRMS (ESI(+)-QTOF): *m*/*z* found 781.1393 $[M + Na]^+$ $C_{29}H_{35}AuClO_7PNa^+$ requires 781.1372 (ppm = 2.69).

Compound ***2c***. According to the general procedure, **1c** (0.370 g, 0.652 mmol, 1 equiv) and AuCl(tht) (0.209 g, 0.652 mmol, 1 equiv) in CH_2Cl_2 (10 mL). The product was isolated as a colorless oil (0.503 g, 0.503 mmol, 96%); Elemental Analysis (%): calcd for $C_{31}H_{39}AuClO_8P$ C 46.37 H 4.90; found C 46.25 H 4.69; ^{1}H NMR ($CDCl_3$, 400 MHz): 8.03−8.11 (2H, m, 2×O−(C═O)−(*Ar*)C−C*H*−CH−C−P), 7.45−7.57 (12H, m, 2×O−(C═O)−(*Ar*)C−CH−C*H*−C−P, 4×P−(*Ar*)C−C*H*−CH−CH, 4×P−(*Ar*)C−CH−C*H*−CH, 2×P−(*Ar*)C−CH−CH−C*H*), 4.45−4.47 (2H m, *Ar*−(C═O)−O−CH_2−CH_2−O), 3.78−3.81 (2H, m, *Ar*−(C═O)−O−CH_2−CH_2−O), 3.53−3.67 (20H, m, *Ar*−(C═O)−O−$(CH_2)_2$−O−(CH_2)$_2$, *Ar*−(C═O)−O−$((CH_2)_2$−O$)_2$−(CH_2)$_2$, *Ar*−(C═O)−O−$((CH_2)_2$−O$)_3$−(CH_2)$_2$, *Ar*−(C═O)−O−$((CH_2)_2$−O$)_4$−(CH_2)$_2$, *Ar*−(C═O)−O−$((CH_2)_2$−O$)_5$−(CH_2)$_2$−OH); ^{31}P {^{1}H} NMR ($CDCl_3$, 162 MHz): 32.98 (1P); ^{13}C {^{1}H} NMR ($CDCl_3$, 101 MHz): 165.4 (1C, O−(C═O)−(*Ar*)C−CH−CH−C−P), 134.2 (1C, d, O−(C═O)−(*Ar*)C−CH−CH−C−P, $^1J_{C,P}$ = 60 Hz), 134.2 (4C, d, 4×P−(*Ar*)C−CH−CH−CH, $^2J_{C,P}$ = 14 Hz), 133.9 (2C, d, 2×O−(C═O)−(*Ar*)C−CH−CH−C−P, $^2J_{C,P}$ = 14 Hz), 133.3 (1C, O−(C═O)−(*Ar*)C−CH−CH−C−P, $^4J_{C,P}$ = 3 Hz), 132.4 (2C, 2×P−(*Ar*)C−CH−CH−CH, $^4J_{C,P}$ = 3 Hz), 130.2 (2C, d, 2×O−(C═O)−(Ar)C−CH−CH−C−P, $^3J_{C,P}$ = 12 Hz), 129.5 (4C, 4×P−(*Ar*)C−CH−CH−CH, $^3J_{C,P}$ = 12 Hz), 127.9 (2C, d, 2×P−(*Ar*)C−CH−CH−CH, $^1J_{C,P}$ = 63 Hz), 72.7 (1C, O−CH_2−CH_2−OH), 70.4−70.6 (7C, *Ar*−(C═O)−O−$(CH_2)_2$−O−CH_2-CH_2, *Ar*−(C═O)−O−$((CH_2)_2$−O$)_2$−(CH_2)$_2$, *Ar*−(C═O)−O−$((CH_2)_2$−O$)_3$−(CH_2)$_2$, *Ar*−(C═O)−O−$((CH_2)_2$−O$)_4$−(CH_2)$_2$), 70.1 (1C, *Ar*−(C═O)−O−$(CH_2)_2$−O−CH_2), 69.1 (1C, *Ar*−(C═O)−O−CH_2−CH_2), 64.7 (1C, *Ar*−(C═O)−O−CH_2−CH_2), 61.6 (1C, O−CH_2−CH_2−OH); HRMS (ESI(+)-QTOF): *m*/*z* found 825.1644 $[M + Na]^+$ $C_{31}H_{39}AuClO_8PNa^+$ requires 825.1635 (ppm = 1.09).

Compound ***2d***. According to the general procedure, **1d** (0.309 g, 0.469 mmol, 1 equiv) and AuCl(tht) (0.150 g, 0.469 mmol, 1 equiv) in CH_2Cl_2 (10 mL). The product was isolated as a colorless oil (0.411 g, 0.461 mmol, 98%); Elemental Analysis (%): calcd for $C_{35}H_{47}AuClO_{10}P$ C 47.17 H 5.32; found C 47.06 H 5.39; ^{1}H NMR ($CDCl_3$, 400 MHz): 8.05−8.07 (2H, m, 2×O−(C═O)−(*Ar*)C−C*H*−CH−C−P), 7.44−7.54 (12H, m, 2×O−(C═O)−(*Ar*)C−CH−C*H*−C−P, 4×P−(*Ar*)C−C*H*−CH−CH, 4×P−(*Ar*)C−CH−C*H*−CH, 2×P−(*Ar*)C−CH−CH−C*H*), 4.42−4.44 (2H m, *Ar*−(C═O)−O−CH_2−CH_2−O), 3.76−3.78 (2H, m, *Ar*−(C═O)−O−CH_2−CH_2−O), 3.52−3.66 (28H, m, *Ar*−(C═O)−O−$(CH_2)_2$−O−(CH_2)$_2$, *Ar*−(C═O)−O−$((CH_2)_2$−O$)_2$−(CH_2)$_2$, *Ar*−(C═O)−O−$((CH_2)_2$−O$)_3$−(CH_2)$_2$, *Ar*−(C═O)−O−$((CH_2)_2$−O$)_4$−(CH_2)$_2$, *Ar*−(C═O)−O−$((CH_2)_2$−O$)_5$−(CH_2)$_2$, *Ar*−(C═O)−O−$((CH_2)_2$−O$)_6$−(CH_2)$_2$, *Ar*−(C═O)−O−$((CH_2)_2$−O$)_7$−(CH_2)$_2$); ^{31}P {^{1}H} NMR ($CDCl_3$, 162 MHz): 32.95 (1P); ^{13}C {^{1}H} NMR ($CDCl_3$, 101 MHz): 165.2 (1C, O−(C═O)−(*Ar*)C−CH−CH−C−P), 134.1 (1C, d, O−(C═O)−(*Ar*)C−CH−CH−C−P, $^1J_{C,P}$ = 60 Hz), 134.1 (4C, d, 4×P−(*Ar*)C−CH−CH−CH, $^2J_{C,P}$ = 14 Hz), 133.8 (2C, d, 2×O−(C═O)−(*Ar*)C−CH−CH−C−P, $^2J_{C,P}$ = 14 Hz), 133.1 (1C, O−(C═O)−(*Ar*)C−CH−CH−C−P, $^4J_{C,P}$ = 3 Hz), 132.3 (2C, 2×P−(*Ar*)C−CH−CH−CH, $^4J_{C,P}$ = 3 Hz), 130.0 (2C, d, 2×O−(C═O)−(Ar)C−CH−CH−C−P, $^3J_{C,P}$ = 12 Hz), 129.3 (4C, 4×P−(*Ar*)C−CH−CH−CH, $^3J_{C,P}$ = 12 Hz), 127.7 (2C, d, 2×P−(*Ar*)C−CH−CH−CH, $^1J_{C,P}$ = 63 Hz), 72.4 (1C, O−CH_2−CH_2−OH), 70.4−70.5 (11C, *Ar*−(C═O)−O−$(CH_2)_2$−O−CH_2-CH_2, *Ar*−(C═O)−O−$((CH_2)_2$−O$)_2$−(CH_2)$_2$, *Ar*−(C═O)−O−$((CH_2)_2$−O$)_3$−(CH_2)$_2$, *Ar*−(C═O)−O−$((CH_2)_2$−O$)_4$−(CH_2)$_2$, *Ar*−(C═O)−O−$((CH_2)_2$−O$)_5$−(CH_2)$_2$, *Ar*−(C═O)−O−$((CH_2)_2$−O$)_6$−(CH_2)$_2$), 70.1 (1C, *Ar*−(C═O)−O−$(CH_2)_2$−O−CH_2), 68.9 (1C, *Ar*−(C═O)−O−CH_2−CH_2), 64.6 (1C, *Ar*−(C═O)−O−CH_2−CH_2), 61.5 (1C, O−CH_2−CH_2−OH); HRMS (ESI-(+)-QTOF): *m*/*z* found 913.2172 $[M + Na]^+$ $C_{35}H_{47}AuClO_{10}PNa^+$ requires 913.2159 (ppm = 1.42).

General Procedure for ***3a−3d***. 4-(Diphenylphosphino)benzoic acid (1.2 equiv) and EDCI (1.5 equiv) were dissolved in dry CH_2Cl_2 (2 mL) and stirred under N_2 at room temperature for 1 h. The solution was added to a solution of the appropriate monophosphine gold(I) complex (1 equiv) and DMAP (0.5 equiv) in dry CH_2Cl_2 (3 mL), and the reaction mixture was stirred under N_2 at room temperature for 20 h. The reaction mixture was washed with brine (40 mL), dried over anhydrous sodium sulfate, filtered, and concentrated under reduced pressure. Purification was achieved via flash column chromatography using an eluent system of CH_2Cl_2/CH_3OH. The product was washed with pentane (3 × 25 mL) and isolated as a cream oil.

DOI: 10.1021/acs.inorgchem.8b03069
Inorg. Chem. 2019, 58, 2501−2513

Compound ***3a***. According to the general procedure, 4-(diphenylphosphino)benzoic acid (0.097 g, 0.317 mmol, 1.2 equiv), EDCI (0.097 g, 0.397 mmol, 1.5 equiv), **2a** (0.189 g, 0.264 mmol, 1 equiv) and DMAP (0.016 g, 0.132 mmol, 0.5 equiv) in CH_2Cl_2 (5 mL). The product was isolated as a cream oil (0.220 g, 0.219 mmol, 83%); Elemental Analysis (%): calcd for $C_{46}H_{44}AuClO_7P_2.^{1/2}CH_2Cl_2$ C 53.41 H 4.34; found C 53.07 H 4.46; ^{1}H NMR ($CDCl_3$, 400 MHz): 7.87–7.89 (4H, m, 4×O–(C═O)–(*Ar*)C–C*H*–CH–C–P), 7.28–7.43 (24H, m, 4×O–(C═O)–(*Ar*)C–CH–C*H*–C–P, 8×P–(*Ar*)C–C*H*–CH–CH, 8×P–(*Ar*)C–CH–C*H*–CH, 4×P–(*Ar*)C–CH–CH–C*H*), 5.29 (s, residual CH_2Cl_2), 4.43–4.46 (4H m, *Ar*–(C═O)–O–CH_2–CH_2–O), 3.79–3.82 (4H, m, *Ar*–(C═O)–O–CH_2–CH_2–O), 3.66–3.68 (8H, m, 2×*Ar*–(C═O)–O–$(CH_2)_2$–O–(CH_2)$_2$); ^{31}P {^{1}H} NMR ($CDCl_3$, 162 MHz): 29.53 (1P); ^{13}C {^{1}H} NMR ($CDCl_3$, 101 MHz): 165.8 (2C, 2×O–(*C*═O)–(*Ar*)C–CH–CH–C–P), 138.6 (2C, d, 2×O–(C═O)–(*Ar*)C–CH–CH–*C*–P, $^1J_{C,P}$ = 33 Hz), 134.1 (8C, 8×P–(*Ar*)C–*C*H–CH–CH), 133.5 (4C, 4×O–(C═O)–(*Ar*)C–CH–*C*H–C–P), 131.8 (2C, 2×O–(C═O)–(*Ar*)*C*–CH–CH–C–P), 131.5 (4C, d, 4×P–(*Ar*)*C*–CH–CH–CH, $^1J_{C,P}$ = 38 Hz), 131.0 (4C, 4×P–(*Ar*)C–CH–CH–*C*H), 129.7 (4C, 4×O–(C═O)–(Ar)C–*C*H–CH–C–P), 129.1 (8C, 8×P–(*Ar*)C–CH–*C*H–CH), 128.8 (2C, d, 2×P–(*Ar*)*C*–CH–CH–CH, $^1J_{C,P}$ = 12 Hz), 70.7–70.8 (4C, 2×*Ar*–(C═O)–O–$(CH_2)_2$–(*C*H_2)$_2$), 69.2 (2C, *Ar*–(C═O)–O–CH_2–*C*H_2), 64.7 (2C, *Ar*–(C═O)–O–*C*H_2–CH_2), 53.5 (residual CH_2Cl_2); HRMS (ESI-(+)-QTOF): *m*/*z* found 967.2210 [M-Cl]$^+$ $C_{46}H_{44}AuO_7P_2^+$ requires 967.2228 (ppm = −1.86).

Compound ***3b***. According to the general procedure, 4-(diphenylphosphino)benzoic acid (0.073 g, 0.237 mmol, 1.2 equiv), EDCI (0.057 g, 0.296 mmol, 1.5 equiv), **2b** (0.150 g, 0.198 mmol, 1 equiv), and DMAP (0.012 g, 0.099 mmol, 0.5 equiv) in CH_2Cl_2 (5 mL). The product was isolated as a cream oil (0.185 g, 0.177 mmol, 89%); Elemental Analysis (%): calcd for $C_{48}H_{48}AuClO_8P_2.^1/_2CH_2Cl_2$ C 53.46 H 4.53; found C 53.27 H 4.76; ^{1}H NMR ($CDCl_3$, 400 MHz): 7.90–7.92 (4H, m, 4×O–(C═O)–(*Ar*)C–C*H*–CH–C–P), 7.29–7.43 (24H, m, 4×O–(C═O)–(*Ar*)C–CH–C*H*–C–P, 8×P–(*Ar*)C–C*H*–CH–CH, 8×P–(*Ar*)C–CH–C*H*–CH, 4×P–(*Ar*)C–CH–CH–C*H*), 4.44–4.46 (4H m, *Ar*–(C═O)–O–CH_2–CH_2–O), 3.79–3.81 (4H, m, *Ar*–(C═O)–O–CH_2–CH_2–O), 3.54–3.59 (12H, m, 2×*Ar*–(C═O)–O–$(CH_2)_2$–O–(CH_2)$_2$, *Ar*–(C═O)–O–$((CH_2)_2$–O$)_2$–(CH_2)$_2$); ^{31}P {^{1}H} NMR ($CDCl_3$, 162 MHz): 31.78 (1P); ^{13}C {^{1}H} NMR ($CDCl_3$, 101 MHz): 165.7 (2C, 2×O–(*C*═O)–(*Ar*)C–CH–CH–C–P), 137.9 (2C, d, 2×O–(C═O)–(*Ar*)C–CH–CH–*C*–P, $^1J_{C,P}$ = 36 Hz), 134.0 (8C, 8×P–(*Ar*)C–*C*H–CH–CH), 133.5 (4C, 4×O–(C═O)–(*Ar*)C–CH–*C*H–C–P), 132.1 (2C, 2×O–(C═O)–(*Ar*)*C*–CH–CH–C–P), 131.4 (4C, 4×P–(*Ar*)C–CH–CH–*C*H), 130.9 (4C, d, 4×P–(*Ar*)*C*–CH–CH–CH, $^1J_{C,P}$ = 40 Hz), 129.9 (4C, 4×O–(C═O)–(Ar)C–*C*H–CH–C–P), 129.3 (8C, 8×P–(*Ar*)C–CH–*C*H–CH), 70.7–70.8 (6C, 2×*Ar*–(C═O)–O–$(CH_2)_2$–(*C*H_2)$_2$, *Ar*–(C═O)–O–$((CH_2)_2$–O$)_2$–(*C*H_2)$_2$), 69.2 (2C, *Ar*–(C═O)–O–CH_2–*C*H_2), 64.7 (2C, *Ar*–(C═O)–O–*C*H_2–CH_2); HRMS (ESI(+)-QTOF): *m*/*z* found 1011.2484 [M-Cl]$^+$ $C_{48}H_{48}AuO_8P_2^+$ requires 1011.2490 (ppm = −0.59).

Compound ***3c***. According to the general procedure, 4-(diphenylphosphino)benzoic acid (0.082 g, 0.269 mmol, 1.2 equiv), EDCI (0.064 g, 0.336 mmol, 1.5 equiv), **2c** (0.180 g, 0.224 mmol, 1 equiv) and DMAP (0.014 g, 0.112 mmol, 0.5 equiv) in CH_2Cl_2 (5 mL). The product was isolated as a cream oil (0.174 g, 0.150 mmol, 62%); Elemental Analysis (%): calcd for $C_{50}H_{52}AuClO_9P_2.\ ^{1/2}C_5H_{12}$ C 55.93 H 5.19; found C 56.14 H 5.04; ^{1}H NMR ($CDCl_3$, 400 MHz): 7.89–7.91 (4H, m, 4×O–(C═O)–(*Ar*)C–C*H*–CH–C–P), 7.28–7.44 (24H, m, 4×O–(C═O)–(*Ar*)C–CH–C*H*–C–P, 8×P–(*Ar*)C–C*H*–CH–CH, 8×P–(*Ar*)C–CH–C*H*–CH, 4×P–(*Ar*)C–CH–CH–C*H*), 5.29 (s, residual CH_2Cl_2), 4.44–4.47 (4H m, *Ar*–(C═O)–O–CH_2–CH_2–O), 3.80–3.82 (4H, m, *Ar*–(C═O)–O–CH_2–CH_2–O), 3.59–3.68 (16H, m, 2×*Ar*–(C═O)–O–$(CH_2)_2$–O–(CH_2)$_2$, 2×*Ar*–(C═O)–O–$((CH_2)_2$–O$)_2$–(CH_2)$_2$); ^{31}P {^{1}H} NMR ($CDCl_3$, 162 MHz): 28.20 (1P); ^{13}C {^{1}H} NMR ($CDCl_3$, 101 MHz): 165.9 (2C, 2×O–(*C*═O)–(*Ar*)C–CH–CH–C–P), 138.6 (2C, d, 2×O–(C═O)–(*Ar*)C–CH–CH–*C*–P, $^1J_{C,P}$ = 32 Hz), 134.1 (8C, 8×P–(*Ar*)C–*C*H–CH–CH), 133.5 (4C, 4×O–(C═O)–(*Ar*)C–CH–*C*H–C–P), 131.8 (2C, 2×O–(C═O)–(*Ar*)*C*–CH–CH–C–P), 131.5 (4C, d, 4×P–(*Ar*)*C*–CH–CH–CH, $^1J_{C,P}$ = 36 Hz), 131.1 (4C, 4×P–(*Ar*)C–CH–CH–*C*H), 129.8 (4C, 4×O–(C═O)–(Ar)C–*C*H–CH–C–P), 129.2 (8C, 8×P–(*Ar*)C–CH–*C*H–CH), 128.8 (2C, d, 2×P–(*Ar*)*C*–CH–CH–CH, $^1J_{C,P}$ = 12 Hz), 70.6–70.8 (8C, 2×*Ar*–(C═O)–O–$(CH_2)_2$–(*C*H_2)$_2$, 2×*Ar*–(C═O)–O–$((CH_2)_2$–O$)_2$–(*C*H_2)$_2$), 69.2 (2C, *Ar*–(C═O)–O–CH_2–*C*H_2), 64.6 (2C, *Ar*–(C═O)–O–*C*H_2–CH_2), 53.5 (residual CH_2Cl_2); HRMS (ESI(+)-QTOF): *m*/*z* found 1055.2816 [M-Cl]$^+$ $C_{50}H_{52}AuO_9P_2^+$ requires 1055.2751 (ppm = 6.16).

Compound ***3d***. According to the general procedure, 4-(diphenylphosphino)benzoic acid (0.066 g, 0.215 mmol, 1.2 equiv), EDCI (0.052 g, 0.269 mmol, 1.5 equiv), **2d** (0.160 g, 0.180 mmol, 1 equiv), and DMAP (0.011 g, 0.090 mmol, 0.5 equiv) in CH_2Cl_2 (5 mL). The product was isolated as a cream oil (0.203 g, 0.172 mmol, 96%); Elemental Analysis (%): calcd for $C_{54}H_{60}AuClO_{11}P_2$ C 54.99 H 5.13; found C54.64 H 5.37; ^{1}H NMR ($CDCl_3$, 400 MHz): 7.90–7.92 (4H, m, 4×O–(C═O)–(*Ar*)C–C*H*–CH–C–P), 7.30–7.46 (24H, m, 4×O–(C═O)–(*Ar*)C–CH–C*H*–C–P, 8×P–(*Ar*)C–C*H*–CH–CH, 8×P–(*Ar*)C–CH–C*H*–CH, 4×P–(*Ar*)C–CH–CH–C*H*), 5.29 (s, residual CH_2Cl_2),4.44–4.47 (4H m, *Ar*–(C═O)–O–CH_2–CH_2–O), 3.80–3.82 (4H, m, *Ar*–(C═O)–O–CH_2–CH_2–O), 3.59–3.70 (24H, m, 2×*Ar*–(C═O)–O–$(CH_2)_2$–O–(CH_2)$_2$, 2×*Ar*–(C═O)–O–$((CH_2)_2$–O$)_2$–(CH_2)$_2$, 2×*Ar*–(C═O)–O–$((CH_2)_2$–O$)_3$–(CH_2)$_2$); ^{31}P {^{1}H} NMR ($CDCl_3$, 162 MHz): 31.09 (1P); ^{13}C {^{1}H} NMR ($CDCl_3$, 101 MHz): 165.7 (2C, 2×O–(*C*═O)–(*Ar*)C–CH–CH–C–P), 137.8 (2C, d, 2×O–(C═O)–(*Ar*)C–CH–CH–*C*–P, $^1J_{C,P}$ = 36 Hz), 134.1 (8C, 8×P–(*Ar*)C–*C*H–CH–CH), 133.5 (4C, 4×O–(C═O)–(*Ar*)C–CH–*C*H–C–P), 132.1 (2C, 2×O–(C═O)–(*Ar*)*C*–CH–CH–C–P), 131.4 (4C, 4×P–(*Ar*)C–CH–CH–*C*H), 130.8 (4C, d, 4×P–(*Ar*)*C*–CH–CH–CH, $^1J_{C,P}$ = 39 Hz), 129.9 (4C, 4×O–(C═O)–(Ar)C–*C*H–CH–C–P), 129.3 (8C, 8×P–(*Ar*)C–CH–*C*H–CH), 128.8 (2C, d, 2×P–(*Ar*)*C*–CH–CH–CH, $^1J_{C,P}$ = 12 Hz), 70.6–70.8 (12C, 2×*Ar*–(C═O)–O–$(CH_2)_2$–(*C*H_2)$_2$, 2×*Ar*–(C═O)–O–$((CH_2)_2$–O$)_2$–(*C*H_2)$_2$, 2×*Ar*–(C═O)–O–$((CH_2)_2$–O$)_3$–(*C*H_2)$_2$), 69.2 (2C, *Ar*–(C═O)–O–CH_2–*C*H_2), 64.7 (2C, *Ar*–(C═O)–O–*C*H_2–CH_2), 53.6 (s, residual CH_2Cl_2); HRMS (ESI-(+)-QTOF): *m*/*z* found 1143.3398 [M-Cl]$^+$ $C_{54}H_{60}AuO_{11}P_2^+$ requires 1143.3276 (ppm = 10.67), *m*/*z* found 1201.2952 [M + Na]$^+$ $C_{54}H_{60}AuClO_{11}P_2Na^+$ requires 1201.2863 (ppm = 7.41).

General Procedure for ***4a–4d***. The appropriate bis-phosphine gold(I) complex (2 equiv) and [Ru(η^6-*p*-cymene)Cl_2]$_2$ (1 equiv) were dissolved in CH_2Cl_2 (5 mL) and stirred at rt under N_2 for 42 h. The solvent was removed via rotary evaporation, and purification was achieved via flash column chromatography using CH_2Cl_2/CH_3OH as the eluent system. The product was washed with pentane (3 × 25 mL) and was isolated as an oily, red solid.

Compound ***4a***. According to the general procedure, **3a** (0.23 g, 0.22 mmol, 2 equiv) and [Ru(η^6-*p*-cymene)Cl_2]$_2$ (0.69 g, 0.11 mmol, 1 equiv) in CH_2Cl_2 (5 mL). The product was isolated as an oily, red solid (0.064 g, 0.049 mmol, 29%); Elemental Analysis (%): calcd for $C_{56}H_{58}AuCl_3O_7P_2Ru{\cdot}CH_2Cl_2$ C 49.10 H 4.34; found C 49.25 H 4.37; ^{1}H NMR ($CDCl_3$, 400 MHz): 8.09–8.11 (2H, m, 2×O–(C═O)–(*Ar*)C–C*H*–CH–C–P–Au), 7.89–7.93 (4H, m, 2×O–(C═O)–(*Ar*)C–C*H*–CH–C–P–Ru, 2×O–(C═O)–(*Ar*)C–CH–C*H*–C–P–Ru), 7.77–7.82 (4H, m, 4×(*Ar*)C–CH–C*H*–C–P–Ru), 7.47–7.56 (12H, m, 2×O–(C═O)–(*Ar*)C–CH–C*H*–C–P–Au, 4×(*Ar*)CH–CH–C*H*–C–P–Au, 4×(*Ar*)CH–C*H*–CH–C–P–Au, 2×(*Ar*)C*H*–CH–CH–C–P–Au), 7.37–7.41 (6H, m, 4×(*Ar*)CH–C*H*–CH–C–P–Ru, 2×(*Ar*)C*H*–CH–CH–C–P–Ru), 5.20–5.21 (2H, d, 2×CH_3–(*Ar*)C–C*H*–CH–C, $^3J_{H,H}$ = 6.1 Hz), 4.98–4.98 (2H, d, 2×CH_3–(*Ar*)C–CH–C*H*–C, $^3J_{H,H}$ = 5.9 Hz), 4.45–4.48 (2H, m, Au–P–*Ar*–(C═O)–O–CH_2–CH_2–O), 4.39–4.42 (2H, m, Ru–P–*Ar*–(C═O)–O–CH_2–CH_2–O), 3.74–3.81 (4H, m, Au–P–*Ar*–(C═O)–O–CH_2–CH_2–O, Ru–P–*Ar*–(C═O)–O–

DOI: 10.1021/acs.inorgchem.8b03069
Inorg. Chem. 2019, 58, 2501–2513

CH_2–CH_2–O), 3.63–3.67 (8H, m, 2×*Ar*–(C=O)–O–$(CH_2)_2$–O–(CH_2)$_2$), 2.80–2.86 (1H, sept, (*Ar*)C–CH–CH–C–C*H*$(CH_3)_2$, $^3J_{H,H}$ = 6.9 Hz), 1.85 (3H, s, CH_3–(*Ar*)C–C*H*–CH–C), 1.09–1.10 (6H, d, (*Ar*)C–CH–CH–C–CH(CH_3)$_2$, $^3J_{H,H}$ = 6.9 Hz); ^{31}P {^{1}H} NMR ($CDCl_3$, 162 MHz): 33.02 (Au–P, 1P), 25.03 (Ru–P, 1P); ^{13}C {^{1}H} NMR ($CDCl_3$, 101 MHz): 166.1 (1C, O–(C=O)–(*Ar*)C–CH–CH–C–P–Ru), 165.4 (1C, O–(C=O)–(*Ar*)C–CH–CH–C–P–Au), 139.05–139.58 (2C, m, O–(C=O)–(*Ar*)C–CH–CH–C–P–Ru, O–(C=O)–(*Ar*)C–CH–CH–C–P–Au), 133.95–134.70 (12C, m, 4×Ru–P–(*Ar*)C–CH–CH–CH, 4×Au–P–(*Ar*)C–CH–CH–CH, 2×O–(C=O)–(*Ar*)C–CH–CH–C–P–Ru, 2×O–(C=O)–(*Ar*)C–CH–CH–C–P–Au), 133.15–133.60 (3C, m, O–(C=O)–(*Ar*)C–CH–CH–C–P–Au, 2×Ru–P–(*Ar*)-C–CH–CH–CH), 132.4 (2C, d, 2×Au–P–(*Ar*)C–CH–CH–CH, $^4J_{C,P}$ = 3 Hz), 131.3 (1C, O–(C=O)–(*Ar*)C–CH–CH–C–P–Ru), 130.7 (2C, 2×Ru–P–(*Ar*)C–CH–CH–CH), 130.1 (2C, 2×O–(C=O)–(Ar)C–CH–CH–C–P–Au), 129.5 (4C, d, 2×Au–P–(*Ar*)C–CH–CH–CH, $^3J_{C,P}$ = 12 Hz), 128.7 (2C, O–(C=O)–(*Ar*)C–CH–CH–C–P–Ru), 128.2 (4C 2×Ru–P–(*Ar*)C–CH–CH–CH), 127.8 (2C, m, 2×Au–P–(*Ar*)C–CH–CH–CH), 111.4 (1C, CH_3–(*Ar*)C–CH–CH–C), 96.4 (1C, CH_3–(*Ar*)C–CH–CH–C), 89.1 (2C, CH_3–(*Ar*)C–CH–CH–C), 87.4 (2C, CH_3–(*Ar*)C–CH–CH–C), 70.71–70.79 (4C, Ru–P–*Ar*–(C=O)–O–$(CH_2)_2$–O–(CH_2)$_2$, Au–P–*Ar*–(C=O)–O–$(CH_2)_2$–O–(CH_2)$_2$), 69.2 (1C, Ru–P–*Ar*–(C=O)–O–CH_2–CH_2), 69.1 (1C, Au–P–*Ar*–(C=O)–O–CH_2–CH_2), 64.7 (1C, Au–P–*Ar*–(C=O)–O–CH_2–CH_2), 64.4 (1C, Ru–P–*Ar*–(C=O)–O–CH_2–CH_2), 30.4 (1C, (*Ar*)C–CH–CH–C–CH–$(CH_3)_2$), 22.0 (2C, (*Ar*)C–CH–CH–C–CH–(CH_3)$_2$), 17.9 (1C, CH_3–(*Ar*)C–CH–CH–C); HRMS (ESI(+)–Orbitrap): *m*/*z* found 1331.1259 $[M + Na]^+$ $C_{56}H_{58}AuCl_3NaO_7P_2Ru^+$ requires 1331.1323 (ppm = −4.78).

Compound ***4b***. According to the general procedure, **3b** (0.14 g, 0.14 mmol, 2 equiv) and $[Ru(\eta^6\text{-}p\text{-cymene})Cl_2]_2$ (0.043 g, 0.069 mmol, 1 equiv) in CH_2Cl_2 (5 mL). The product was isolated as an oily, red solid (0.078 g, 0.058 mmol, 41%); Elemental Analysis (%): calcd for $C_{58}H_{62}AuCl_3O_8P_2Ru{\cdot}CH_2Cl_2$ C 49.27 H 4.49; found C 49.19 H 4.51; ^{1}H NMR ($CDCl_3$, 400 MHz): 8.10–8.12 (2H, m, 2×O–(C=O)–(*Ar*)C–C*H*–CH–C–P–Au), 7.90–7.95 (4H, m, 2×O–(C=O)–(*Ar*)C–C*H*–CH–C–P–Ru, 2×O–(C=O)–(*Ar*)C–CH–C*H*–C–P–Ru), 7.78–7.83 (4H, m, 4×(*Ar*)C–CH–C*H*–C–P–Ru), 7.53–7.57 (12H, m, 2×O–(C=O)–(*Ar*)C–CH–C*H*–C–P–Au, 4×(*Ar*)CH–CH–C*H*–C–P–Au, 4×(*Ar*)CH–C*H*–CH–C–P–Au, 2×(*Ar*)C*H*–CH–CH–C–P–Au), 7.38–7.50 (6H, m, 4×(*Ar*)CH–C*H*–CH–C–P–Ru, 2×(*Ar*)C*H*–CH–CH–C–P–Ru), 5.21–5.22 (2H, d, 2×CH_3–(*Ar*)C–C*H*–CH–C, $^3J_{H,H}$ = 6.2 Hz), 4.97–4.99 (2H, d, 2×CH_3–(*Ar*)C–CH–C*H*-C, $^3J_{H,H}$ = 5.9 Hz), 4.46–4.49 (2H, m, Au–P–*Ar*–(C=O)–O–CH_2–CH_2–O), 4.41–4.43 (2H, m, Ru–P–*Ar*–(C=O)–O–CH_2–CH_2–O), 3.76–3.82 (4H, m, Au–P–*Ar*–(C=O)–O–CH_2–CH_2–O, Ru–P–*Ar*–(C=O)–O–CH_2–CH_2–O), 3.61–3.68 (12H, m, 2×*Ar*–(C=O)–O–$(CH_2)_2$–O–(CH_2)$_2$, 2×*Ar*–(C=O)–O–((CH_2)$_2$–O)$_2$-CH_2), 2.83–2.87 (1H, sept, (*Ar*)C–CH–CH–C–C*H*$(CH_3)_2$, $^3J_{H,H}$ = 6.9 Hz), 1.86 (3H, s, CH_3–(*Ar*)C–C*H*–CH–C), 1.10–1.12 (6H, d, (*Ar*)C–CH–CH–C–CH$(CH_3)_2$, $^3J_{H,H}$ = 6.9 Hz); ^{31}P {^{1}H} NMR ($CDCl_3$, 162 MHz): 33.02 (Au–P, 1P), 25.00 (Ru–P, 1P); ^{13}C {^{1}H} NMR ($CDCl_3$, 101 MHz): 166.1 (1C, O–(C=O)–(*Ar*)C–CH–CH–C–P–Ru), 165.4 (1C, O–(C=O)–(*Ar*)C–CH–CH–C–P–Au), 139.09–139.61 (2C, m, O–(C=O)–(*Ar*)C–CH–CH–C–P–Ru, O–(C=O)–(*Ar*)C–CH–CH–C–P–Au), 133.99–134.71 (12C, m, 4×Ru–P–(*Ar*)C–CH–CH–CH, 4×Au–P–(*Ar*)C–CH–CH–CH, 2×O–(C=O)–(*Ar*)C–CH–CH–C–P–Ru, 2×O–(C=O)–(*Ar*)C–CH–CH–C–P–Au), 133.18–133.68 (3C, m, O–(C=O)–(*Ar*)C–CH–CH–C–P–Au, 2×Ru–P–(*Ar*)-C–CH–CH–CH), 132.4 (2C, d, 2×Au–P–(*Ar*)C–CH–CH–CH, $^4J_{C,P}$ = 3 Hz), 131.3 (1C, O–(C=O)–(*Ar*)C–CH–CH–C–P–Ru), 130.7 (2C, 2×Ru–P–(*Ar*)C–CH–CH–CH), 130.1 (2C, d, 2×O–(C=O)–(Ar)C–CH–CH–C–P–Au, $^3J_{C,P}$ = 12 Hz), 129.6 (4C, d, 2×Au–P–(*Ar*)C–CH–CH–CH, $^3J_{C,P}$ = 12 Hz), 128.8 (2C, O–(C=O)–(*Ar*)C–CH–CH–C–P–Ru), 128.3 (4C 2×Ru–P–(*Ar*)C–CH–CH–CH), 127.8 (2C, m, 2×Au–P–(*Ar*)C–CH–CH–CH–CH), 111.6 (1C, CH_3–(*Ar*)C–CH–CH–C), 96.4 (1C, CH_3–(*Ar*)C–CH–CH–C), 89.1 (2C, CH_3–(*Ar*)C–CH–CH–C), 87.5 (2C, CH_3–(*Ar*)C–CH–CH–C), 70.71–70.78 (6C, Ru–P–*Ar*–(C=O)–O–$(CH_2)_2$–O–$(CH_2)_2$, Au–P–*Ar*–(C=O)–O–$(CH_2)_2$–O–$(CH_2)_2$), Ru–P–*Ar*–(C=O)–O–((CH_2)$_2$–O)$_2$-CH_2, Au–P–*Ar*–(C=O)–O–((CH_2)$_2$–O)$_2$-CH_2), 69.2 (1C, Ru–P–*Ar*–(C=O)–O–CH_2–CH_2), 69.1 (1C, Au–P–*Ar*–(C=O)–O–CH_2–CH_2), 64.8 (1C, Au–P–*Ar*–(C=O)–O–CH_2–CH_2), 64.5 (1C, Ru–P–*Ar*–(C=O)–O–CH_2–CH_2), 30.4 (1C, (*Ar*)C–CH–CH–C–CH–$(CH_3)_2$), 22.0 (2C, (*Ar*)C–CH–CH–C–CH–$(CH_3)_2$), 17.9 (1C, CH_3–(*Ar*)C–CH–CH–C); HRMS (ESI(+)-QTOF): *m*/*z* found 1317.1989 $[M - Cl]^+$ $C_{58}H_{62}AuCl_2O_8P_2Ru^+$ requires 1317.2017 (ppm = −2.13).

Compound ***4c***. According to the general procedure, **3c** (0.20 g, 0.18 mmol, 2 equiv) and $[Ru(\eta^6\text{-}p\text{-cymene})Cl_2]_2$ (0.056 g, 0.091 mmol, 1 equiv) in CH_2Cl_2 (5 mL). The product was isolated as an oily, red solid (0.036 g, 0.025 mmol, 14%); Elemental Analysis (%): calcd for $C_{60}H_{66}AuCl_3O_9P_2Ru{\cdot}C_5H_{12}$ C 53.12 H 5.35; found C 52.96 H 5.35; ^{1}H NMR ($CDCl_3$, 400 MHz): 8.09–8.12 (2H, m, 2×O–(C=O)–(*Ar*)C–C*H*–CH–C–P–Au), 7.89–7.94 (4H, m, 2×O–(C=O)–(*Ar*)C–C*H*–CH–C–P–Ru, 2×O–(C=O)–(*Ar*)C–CH–C*H*–C–P–Ru), 7.78–7.82 (4H, m, 4×(*Ar*)C–CH–C*H*–C–P–Ru), 7.52–7.59 (12H, m, 2×O–(C=O)–(*Ar*)C–CH–C*H*–C–P–Au, 4×(*Ar*)CH–CH–C*H*–C–P–Au, 4×(*Ar*)CH–C*H*–CH–C–P–Au, 2×(*Ar*)C*H*–CH–CH–C–P–Au), 7.37–7.49 (6H, m, 4×(*Ar*)CH–C*H*–CH–C–P–Ru, 2×(*Ar*)C*H*–CH–CH–C–P–Ru), 5.20–5.22 (2H, d, 2×CH_3–(*Ar*)C–C*H*–CH–C, $^3J_{H,H}$ = 5.9 Hz), 4.97–4.98 (2H, d, 2×CH_3–(*Ar*)C–CH–C*H*–C, $^3J_{H,H}$ = 5.6 Hz), 4.46–4.49 (2H, m, Au–P–*Ar*–(C=O)–O–CH_2–CH_2–O), 4.40–4.43 (2H, m, Ru–P–*Ar*–(C=O)–O–CH_2–CH_2–O), 3.76–3.82 (4H, m, Au–P–*Ar*–(C=O)–O–CH_2–CH_2–O, Ru–P–*Ar*–(C=O)–O–CH_2–CH_2–O), 3.58–3.68 (16H, m, 2×*Ar*–(C=O)–O–$(CH_2)_2$–O–(CH_2)$_2$, 2×*Ar*–(C=O)–O–((CH_2)$_2$–O)$_2$–(CH_2)$_2$), 2.83–2.86 (1H, sept, (*Ar*)C–CH–CH–C–C*H*$(CH_3)_2$, $^3J_{H,H}$ = 6.9 Hz), 1.85 (3H, s, CH_3–(*Ar*)C–C*H*–CH–C), 1.09–1.11 (6H, d, (*Ar*)C–CH–CH–C–CH(CH_3)$_2$, $^3J_{H,H}$ = 6.9 Hz); ^{31}P {^{1}H} NMR ($CDCl_3$, 162 MHz): 33.02 (Au–P, 1P), 24.99 (Ru–P, 1P); ^{13}C {^{1}H} NMR ($CDCl_3$, 101 MHz): 166.1 (1C, O–(C=O)–(*Ar*)C–CH–CH–C–P–Ru), 165.4 (1C, O–(C=O)–(*Ar*)C–CH–CH–C–P–Au), 139.15–139.58 (2C, m, O–(C=O)–(*Ar*)C–CH–CH–C–P–Ru, O–(C=O)–(*Ar*)C–CH–CH–C–P–Au), 133.60–134.67 (12C, m, 4×Ru–P–(*Ar*)C–CH–CH–CH, 4×Au–P–(*Ar*)C–CH–CH–CH, 2×O–(C=O)–(*Ar*)C–CH–CH–C–P–Ru, 2×O–(C=O)–(*Ar*)C–CH–CH–C–P–Au), 133.15–133.63 (3C, m, O–(C=O)–(*Ar*)C–CH–CH–C–P–Au, 2×Ru–P–(*Ar*)-C–CH–CH–CH), 132.4 (2C, d,2×Au–P–(*Ar*)C–CH–CH–CH, $^4J_{C,P}$ = 3 Hz), 131.3 (1C, O–(C=O)–(*Ar*)C–CH–CH–C–P–Ru), 130.7 (2C, 2×Ru–P–(*Ar*)C–CH–CH–CH), 130.2 (2C, d, 2×O–(C=O)–(Ar)C–CH–CH–C–P–Au, $^3J_{C,P}$ = 12 Hz), 129.5 (4C, d, 2×Au–P–(*Ar*)C–CH–CH–CH, $^3J_{C,P}$ = 12 Hz), 128.8 (2C, O–(C=O)–(*Ar*)C–CH–CH–C–P–Ru), 128.3 (4C, d, 2×Ru–P–(*Ar*)C–CH–CH–CH, $^3J_{C,P}$ = 10 Hz), 127.8 (2C, d, 2×Au–P–(*Ar*)C–CH–CH–CH, $^1J_{C,P}$ = 63 Hz), 111.6 (1C, CH_3–(*Ar*)C–CH–CH–C), 96.4 (1C, CH_3–(*Ar*)C–CH–CH–C), 89.1 (2C, CH_3–(*Ar*)C–CH–CH–C), 87.4 (2C, CH_3–(*Ar*)C–CH–CH–C), 70.68–70.77 (8C, Ru–P–*Ar*–(C=O)–O–$(CH_2)_2$–O–(CH_2)$_2$, Au–P–*Ar*–(C=O)–O–$(CH_2)_2$–O–(CH_2)$_2$), Ru–P–*Ar*–(C=O)–O–((CH_2)$_2$–O)$_2$–(CH_2)$_2$, Au–P–*Ar*–(C=O)–O–((CH_2)$_2$–O)$_2$–(CH_2)$_2$), 69.2 (1C, Ru–P–*Ar*–(C=O)–O–CH_2–CH_2), 69.1 (1C, Au–P–*Ar*–(C=O)–O–CH_2–CH_2), 64.8 (1C, Au–P–*Ar*–(C=O)–O–CH_2–CH_2), 64.5 (1C, Ru–P–*Ar*–(C=O)–O–CH_2–CH_2), 30.4 (1C, (*Ar*)C–CH–CH–C–C*H*–$(CH_3)_2$), 22.0 (2C, (*Ar*)C–CH–CH–C–CH–(CH_3)$_2$), 17.9 (1C, CH_3–(*Ar*)C–CH–CH–C); HRMS (ESI(+)–Orbitrap): *m*/*z* found 1419.1779 $[M + Na]^+$ $C_{60}H_{66}AuCl_3NaO_9P_2Ru^+$ requires 1419.1849 (ppm = −4.93).

Compound ***4d***. According to the general procedure, **3d** (0.21 g, 0.18 mmol, 2 equiv) and $[Ru(\eta^6\text{-}p\text{-cymene})Cl_2]_2$ (0.056 g, 0.091

DOI: 10.1021/acs.inorgchem.8b03069
Inorg. Chem. 2019, 58, 2501–2513

mmol, 1 equiv) in CH_2Cl_2 (5 mL). The product was isolated as an oily, red solid (0.031 g, 0.021 mmol, 11%); Elemental Analysis (%): calcd for $C_{64}H_{74}AuCl_3O_{11}P_2Ru{\cdot}CDCl_3$ C 48.61 H 4.77; found C 48.95 H 4.44; ^{1}H NMR ($CDCl_3$, 400 MHz): 8.10−8.12 (2H, m, 2×O−(C═O)−(*Ar*)C−C*H*−CH−C−P−Au), 7.90−7.94 (4H, m, 2×O−(C═O)−(*Ar*)C−C*H*−CH−C−P−Ru, 2×O−(C═O)−(*Ar*)C−CH−C*H*−C−P−Ru), 7.78−7.83 (4H, m, 4×(*Ar*)C−CH−C*H*−C−P−Ru), 7.53−7.58 (12H, m, 2×O−(C═O)−(*Ar*)C−CH−C*H*−C−P−Au, 4×(*Ar*)CH−CH−C*H*−C−P−Au, 4×(*Ar*)CH−C*H*−CH−C−P−Au, 2×(*Ar*)C*H*−CH−CH−C−P−Au), 7.38−7.50 (6H, m, 4×(*Ar*)CH−C*H*−CH−C−P−Ru, 2×(*Ar*)C*H*−CH−CH−C−P−Ru), 5.20−5.22 (2H, d, 2×CH_3−(*Ar*)C−C*H*−CH−C, $^3J_{H,H}$ = 6.0 Hz), 4.97−4.99 (2H, d, 2×CH_3−(*Ar*)C−CH−C*H*−C, $^3J_{H,H}$ = 6.3 Hz), 4.47−4.50 (2H, m, Au−P−*Ar*−(C═O)−O−CH_2−CH_2−O), 4.41−4.44 (2H, m, Ru−P−*Ar*−(C═O)−O−CH_2−CH_2−O), 3.77−3.83 (4H, m, Au−P−*Ar*−(C═O)−O−CH_2−CH_2−O, Ru−P−*Ar*−(C═O)−O−CH_2−CH_2−O), 3.61−3.65 (24H, m, 2×*Ar*−(C═O)−O−$(CH_2)_2$−O−(CH_2)$_2$, 2×*Ar*−(C═O)−O−$((CH_2)_2$−O$)_2$−(CH_2)$_2$, 2×*Ar*−(C═O)−O−$((CH_2)_2$−O$)_3$−(CH_2)$_2$), 2.81−2.88 (1H, sept, (*Ar*)C−CH−CH−C−C*H*$(CH_3)_2$, $^3J_{H,H}$ = 6.9 Hz), 1.85 (3H, s, CH_3−(*Ar*)C−C*H*−CH−C), 1.10−1.11 (6H, d, (*Ar*)C−CH−CH−C−CH(CH_3)$_2$, $^3J_{H,H}$ = 6.9 Hz); ^{31}P {^{1}H} NMR ($CDCl_3$, 162 MHz): 33.02 (Au−P, 1P), 24.95 (Ru−P, 1P); ^{13}C {^{1}H} NMR ($CDCl_3$, 101 MHz): 166.1 (1C, O−(C═O)−(*Ar*)C−CH−CH−C−P−Ru), 165.4 (1C, O−(C═O)−(*Ar*)C−CH−CH−C−P−Au), 139.13−139.60 (2C, m, O−(C═O)−(*Ar*)C−CH−CH−C−P−Ru, O−(C═O)−(*Ar*)C−CH−CH−C−P−Au), 133.98−134.68 (12C, m, 4×Ru−P−(*Ar*)C−CH−CH−CH, 4×Au−P−(*Ar*)C−CH−CH−CH, 2×O−(C═O)−(*Ar*)C−CH−CH−C−P−Ru, 2×O−(C═O)−(*Ar*)C−CH−CH−C−P−Au), 133.18−133.63 (3C, m, O−(C═O)−(*Ar*)C−CH−CH−C−P−Au, 2×Ru−P−(*Ar*)-C−CH−CH−CH), 132.4 (2C, d, 2×Au−P−(*Ar*)C−CH−CH−CH, $^4J_{C,P}$ = 3 Hz), 131.3 (1C, O−(C═O)−(*Ar*)C−CH−CH−C−P−Ru), 130.7 (2C, d, 2×Ru−P−(*Ar*)C−CH−CH−CH, $^4J_{C,P}$ = 3 Hz), 130.2 (2C, d, 2×O−(C═O)−(Ar)C−CH−CH−C−P−Au, $^3J_{C,P}$ = 12 Hz), 129.5 (4C, d, 2×Au−P−(*Ar*)C−CH−CH−CH, $^3J_{C,P}$ = 12 Hz), 128.8 (2C, d, O−(C═O)−(*Ar*)C−CH−CH−C−P−Ru, $^3J_{C,P}$ = 10 Hz), 128.3 (4C, d, 2×Ru−P−(*Ar*)C−CH−CH−CH, $^3J_{C,P}$ = 10 Hz), 127.8 (2C, d, 2×Au−P−(*Ar*)C−CH−CH−CH, $^1J_{C,P}$ = 63 Hz), 111.6 (1C, CH_3−(*Ar*)C−CH−CH−C), 96.4 (1C, CH_3−(*Ar*)C−CH−CH−C), 89.1 (2C, CH_3−(*Ar*)C−CH−CH−C), 87.4 (2C, CH_3−(*Ar*)C−CH−CH−C), 70.65−70.77 (12C, Ru−P−*Ar*−(C═O)−O−$(CH_2)_2$−O−(CH_2)$_2$, Au−P−*Ar*−(C═O)−O−$(CH_2)_2$−O−(CH_2)$_2$, Ru−P−*Ar*−(C═O)−O−$((CH_2)_2$−O$)_2$−(CH_2)$_2$, Au−P−*Ar*−(C═O)−O−$((CH_2)_2$−O$)_2$−(CH_2)$_2$, Ru−P−*Ar*−(C═O)−O−$((CH_2)_2$−O$)_3$−(CH_2)$_2$, Au−P−*Ar*−(C═O)−O−$((CH_2)_2$−O$)_3$−(CH_2)$_2$), 69.2 (1C, Ru−P−*Ar*−(C═O)−O−CH_2−CH_2), 69.1 (1C, Au−P−*Ar*−(C═O)−O−CH_2−CH_2), 64.8 (1C, Au−P−*Ar*−(C═O)−O−CH_2−CH_2), 64.5 (1C, Ru−P−*Ar*−(C═O)−O−CH_2−CH_2), 30.4 (1C, (*Ar*)C−CH−CH−C−C*H*−$(CH_3)_2$), 22.0 (2C, (*Ar*)C−CH−CH−C−CH−(CH_3)$_2$), 17.9 (1C, CH_3−(*Ar*)C−CH−CH−C); HRMS (ESI(+)−Orbitrap): *m*/*z* found 1507.2302 [M + Na]$^+$ $C_{64}H_{74}AuCl_3NaO_{11}P_2Ru^+$ requires 1507.2375 (ppm = −4.80).

Cell Culture and Cytotoxicity Studies. Human ovarian carcinoma (A2780 and A2780cisR) cell lines were obtained from the European Collection of Cell Cultures. The human embryonic kidney (HEK-293) cell line was obtained from ATCC (Sigma, Buchs, Switzerland). Penicillin streptomycin, RPMI 1640 GlutaMAX (where RPMI = Roswell Park Memorial Institute), and DMEM GlutaMAX media (where DMEM = Dulbecco's modified Eagle's medium) were obtained from Life Technologies, and fetal bovine serum (FBS) was obtained from Sigma. The cells were cultured in RPMI 1640 GlutaMAX (A2780 and A2780cisR) and DMEM GlutaMAX (HEK-293) media containing 10% heat-inactivated FBS and 1% penicillin−streptomycin at 37 °C and CO_2 (5%). The A2780cisR cell line was routinely treated with cisplatin (2 μM) in the media to maintain cisplatin resistance. The cytotoxicity was determined using the 3-(4,5-dimethyl 2-thiazolyl)-2,5-diphenyl-2*H*-tetrazolium bromide (MTT) assay.[43] Cells were seeded in flat-bottomed 96-well plates as a suspension in a prepared medium (100 μL aliquots and approximately 4300 cells/well) and preincubated for 24 h. Stock solutions of compounds were prepared in DMSO and were rapidly diluted in a medium. The solutions were sequentially diluted to give a final DMSO concentration of 0.5% and a final compound concentration range (0−200 μM). Cisplatin and RAPTA-C were tested as positive (0−100 μM) and negative (200 μM) controls, respectively. The compounds were added to the preincubated 96-well plates in 100 μL aliquots, and the plates were incubated for a further 72 h. MTT (20 μL, 5 mg/mL in Dulbecco's phosphate buffered saline) was added to the cells, and the plates were incubated for a further 4 h. The culture medium was aspirated, and the purple formazan crystals, formed by the mitochondrial dehydrogenase activity of vital cells, were dissolved in DMSO (100 μL/well). The absorbance of the resulting solutions, directly proportional to the number of surviving cells, was quantified at 590 nm using a SpectroMax M5e multimode microplate reader (using SoftMax Pro software, version 6.2.2). The percentage of surviving cells was calculated from the absorbance of wells corresponding to the untreated control cells. The reported IC50 values are based on the means from two independent experiments, each comprising four tests per concentration level.

Mass Spectrometry Binding Studies. *Binding Studies of* ***4b*** *with* L*-Histidine.* Complex **4b** was incubated under agitation with L-histidine for 2 h in a 1:1 complex−amino acid ratio in unbuffered solution (98% Milli-Q water, 2% DMSO) at 310 K. The samples were diluted first in millQ water (factor 100) and then in CH_3OH/HCOOH (0.1% HCOOH in CH_3OH) by a factor of 10.

Binding Studies of ***4a*** *and* ***4d*** *with 1−16-mer β-Amyloid Peptide.* Complex **4a** or **4d** was incubated under agitation with the 16-*mer* β-amyloid protein for 2 h in a 1:3 complex−peptide ratio in unbuffered solution (98% Milli-Q, 2% DMSO) at 310 K. The samples were diluted first in millQ water (factor 100) and then in CH_3OH/HCOOH (0.1% HCOOH in CH_3OH) by a factor of 10.

Xevo G2-S QTOF. Routine analyses were conducted on a Xevo G2-S QTOF mass spectrometer coupled to the Acquity UPLC Class Binary Solvent manager and BTN sample manager (Waters, Corporation, Milford, MA). The sample manager system temperature was maintained at 10 °C, and the injection volume was 2 μL. Mass spectrometer detection was operated in positive ionization using the ZSpray dual-orthogonal multimode ESI/APCI/ESCi source. The TOF mass spectra were acquired in the resolution mode over the range of *m*/*z* 50−1200 at an acquisition rate of 0.036 s/spectra. The instrument was calibrated using a solution of sodium formate (0.01 mg/L in isopropanol/H_2O 90:10). A mass accuracy better than 5 ppm was achieved using a Leucine Enkephalin solution as lock-mass (200 pg/mL in ACN/H_2O (50:50)) infused continuously using the LockSpray source. Source settings were as follows: cone, 25 V; capillary, 3 kV, source temperature, 150 °C; desolvation temperature, 500 °C, cone gas, 10 L/h, desolvation gas, 500 L/h. Data were processed using MassLynx 4.1 software and QuanLynx application for quantification.

LTQ Orbitrap FTMS. Mass spectrometry analyses were performed on a LTQ Orbitrap FTMS instrument (LTQ Orbitrap Elite FTMS, Thermo Scientific, Bremen, Germany) operated in the positive mode coupled with a robotic chip-based nano-ESI source (TriVersa Nanomate, Advion Biosciences, Ithaca, NY, United States). A standard data acquisition and instrument control system was utilized (Thermo Scientific), whereas the ion source was controlled by Chipsoft 8.3.1 software (Advion BioScience). Samples were loaded onto a 96-well plate (Eppendorf, Hamburg, Germany) within an injection volume of 5 μL. The experimental conditions for the ionization voltage was +1.4 kV, and the gas pressure was set at 0.30 psi. The temperature of ion transfer capillary was 275 °C and the S-lens value was settled at 67%.. FTMS spectra were obtained in the 200−2000 *m*/*z* range in the reduced profile mode with a resolution set to 120 000. In all spectra, one microscan was acquired with a maximum injection time value of 1000 ms. For CID, ETD and HCD analysis, each precursor ion was isolated with a width window of 8. Normalized collision energies for CID and HCD fragmentation were 30 and 18%, respectively. A total of 100 scans each consisting of 10

DOI: 10.1021/acs.inorgchem.8b03069
Inorg. Chem. 2019, 58, 2501−2513

μscans were acquired in reduced profile mode and averaged. ETD reaction time was set at 180 ms.

General Input Apm²s Parameters. Experimental MS were exported as .txt files before being dropped into the Apm²s tool.[46,51] Protons (+1 to +5), modifiable charge (+1 to +5), and metal adduct ($C_{56}H_{58}AuO_7P_2Ru$) in the different boxes of "List of groups". Zone widths were selected based of the Ru expected isotopic pattern (−6.5 to 8.5), and the common zone parameter was fixed "as second". Minimal similarity was set at 70%, max results at 500, and best result range at 0. b, y, and b/y (internal fragments) fragment ions were selected for the CID experiments, whereas c, z, and c/z were chosen for ETD.

■ ASSOCIATED CONTENT

Supporting Information

The Supporting Information is available free of charge on the ACS Publications website at DOI: 10.1021/acs.inorgchem.8b03069.

(PDF)

■ AUTHOR INFORMATION

Corresponding Author

*E-mail: paul.dyson@epfl.ch.

ORCID

Paul J. Dyson: 0000-0003-3117-3249

Notes

The authors declare no competing financial interest.

■ ACKNOWLEDGMENTS

We thank the Swiss National Science Foundation for their financial support and Dr. Laure Menin for helpful discussions.

■ REFERENCES

(1) Sava, G.; Jaouen, G.; Hillard, E. A.; Bergamo, A. Targeted therapy vs. DNA-adduct formation-guided design: thoughts about the future of metal-based anticancer drugs. *Dalton Trans.* **2012**, *41*, 8226−8234.

(2) Murray, B. S.; Babak, M. V.; Hartinger, C. G.; Dyson, P. J. The development of RAPTA compounds for the treatment of tumors. *Coord. Chem. Rev.* **2016**, *306*, 86−114.

(3) Lee, R. F. S.; Escrig, S.; Croisier, M.; Clerc-Rosset, S.; Knott, G. W.; Meibom, A.; Davey, C. A.; Johnsson, K.; Dyson, P. J. NanoSIMS analysis of an isotopically labelled organometallic ruthenium (II) drug to probe its distribution and state in vitro. *Chem. Commun.* **2015**, *51*, 16486−16489.

(4) Zheng, W.; Zhao, Y.; Luo, Q.; Zhang, Y.; Wu, K.; Wang, F. Rational design of multi-targeting ruthenium-and platinum-based anticancer complexes. *Sci. China: Chem.* **2016**, *59*, 1240−1249.

(5) Adhireksan, Z.; Davey, G. E.; Campomanes, P.; Groessl, M.; Clavel, C. M.; Yu, H.; Nazarov, A. A.; Yeo, C. H. F.; Ang, W. H.; Dröge, P.; Roethlisberger, U.; Dyson, P. J.; Davey, C. A. Ligand substitutions between ruthenium−cymene compounds can control protein versus DNA targeting and anticancer activity. *Nat. Commun.* **2014**, *5*, 3462.

(6) Ma, Z.; Palermo, G.; Adhireksan, Z.; Murray, B. S.; Von Erlach, T.; Dyson, P. J.; Roethlisberger, U.; Davey, C. A. An Organometallic Compound which Exhibits a DNA Topology-Dependent One-Stranded Intercalation Mode. *Angew. Chem., Int. Ed.* **2016**, *55*, 7441−7444.

(7) Wu, B.; Ong, M. S.; Groessl, M.; Adhireksan, Z.; Hartinger, C. G.; Dyson, P. J.; Davey, C. A. A ruthenium antimetastasis agent forms specific histone protein adducts in the nucleosome core. *Chem. - Eur. J.* **2011**, *17*, 3562−3566.

(8) Davey, G. E.; Adhireksan, Z.; Ma, Z.; Riedel, T.; Sharma, D.; Padavattan, S.; Rhodes, D.; Ludwig, A.; Sandin, S.; Murray, B. S.; Dyson, P. J.; Davey, C. A. Nucleosome acidic patch-targeting binuclear ruthenium compounds induce aberrant chromatin condensation. *Nat. Commun.* **2017**, *8*, 1575.

(9) Scolaro, C.; Bergamo, A.; Brescacin, L.; Delfino, R.; Cocchietto, M.; Laurenczy, G.; Geldbach, T. J.; Sava, G.; Dyson, P. J. In vitro and in vivo evaluation of ruthenium (II)− arene PTA complexes. *J. Med. Chem.* **2005**, *48*, 4161−71.

(10) Roder, C.; Thomson, M. J. Auranofin: repurposing an old drug for a golden new age. *Drugs R&D* **2015**, *15*, 13−20.

(11) Adhireksan, Z.; Palermo, G.; Riedel, T.; Ma, Z.; Muhammad, R.; Rothlisberger, U.; Dyson, P. J.; Davey, C. A. Allosteric cross-talk in chromatin can mediate drug-drug synergy. *Nat. Commun.* **2017**, *8*, 14860.

(12) García-Moreno, E.; Gascón, S.; Rodriguez-Yoldi, M. J.; Cerrada, E.; Laguna, M. S-propargylthiopyridine phosphane derivatives as anticancer agents: Characterization and antitumor activity. *Organometallics* **2013**, *32*, 3710−3720.

(13) Barreiro, E.; Casas, J. S.; Couce, M. D.; Sánchez, A.; Sordo, J.; Vázquez-López, E. M. Heteronuclear gold (I)−silver (I) sulfanylcarboxylates: Synthesis, structure and cytotoxic activity against cancer cell lines. *J. Inorg. Biochem.* **2014**, *131*, 68−75.

(14) Wenzel, M.; Bigaeva, E.; Richard, P.; Le Gendre, P.; Picquet, M.; Casini, A.; Bodio, E. New heteronuclear gold (I)−platinum (II) complexes with cytotoxic properties: Are two metals better than one? *J. Inorg. Biochem.* **2014**, *141*, 10−16.

(15) Zaidi, Y.; Arjmand, F.; Zaidi, N.; Usmani, J. A.; Zubair, H.; Akhtar, K.; Hossain, M.; Shadab, G. A comprehensive biological insight of trinuclear copper (ii)−tin (iv) chemotherapeutic anticancer drug entity: in vitro cytotoxicity and in vivo systemic toxicity studies. *Metallomics* **2014**, *6*, 1469−1479.

(16) Singh, N.; Jang, S.; Jo, J.; Kim, D. H.; Park, D. W.; Kim, I.; Kim, H.; Kang, S. C.; Chi, K. Coordination-Driven Self-Assembly and Anticancer Potency Studies of Ruthenium−Cobalt-Based Heterometallic Rectangles. *Chem. - Eur. J.* **2016**, *22*, 16157−16164.

(17) Lopes, J.; Alves, D.; Morais, T. S.; Costa, P. J.; Piedade, M. F. M.; Marques, F.; de Brito, M. J. V.; Garcia, M. H. New copper (I) and heteronuclear copper (I)−ruthenium (II) complexes: synthesis, structural characterization and cytotoxicity. *J. Inorg. Biochem.* **2017**, *169*, 68−78.

(18) Fernández-Moreira, V.; Gimeno, M. C. Heterobimetallic Complexes for Theranostic Applications. *Chem. - Eur. J.* **2018**, *24*, 3345−3353.

(19) Pelletier, F.; Comte, V.; Massard, A.; Wenzel, M.; Toulot, S.; Richard, P.; Picquet, M.; Le Gendre, P.; Zava, O.; Edafe, F. Development of bimetallic titanocene− ruthenium− arene complexes as anticancer agents: relationships between structural and biological properties. *J. Med. Chem.* **2010**, *53*, 6923−6933.

(20) Fernández-Moreira, V.; Marzo, I.; Gimeno, M. C. Luminescent Re (I) and Re (I)/Au (I) complexes as cooperative partners in cell imaging and cancer therapy. *Chem. Sci.* **2014**, *5*, 4434−4446.

(21) Nithyakumar, A.; Alexander, V. Synthesis, relaxivity, and in vitro fluorescence imaging studies of a novel d−f heterometallic trinuclear complex as a potential bimodal imaging probe for MRI and optical imaging. *Dalton Trans.* **2015**, *44*, 17800−17809.

(22) Wenzel, M.; Bertrand, B.; Eymin, M.-J.; Comte, V.; Harvey, J. A.; Richard, P.; Groessl, M.; Zava, O.; Amrouche, H.; Harvey, P. D. Multinuclear cytotoxic metallodrugs: physicochemical characterization and biological properties of novel heteronuclear gold−titanium complexes. *Inorg. Chem.* **2011**, *50*, 9472−9480.

(23) Luengo, A.; Fernández-Moreira, V.; Marzo, I.; Gimeno, M. C. Trackable Metallodrugs Combining Luminescent Re (I) and Bioactive Au (I) Fragments. *Inorg. Chem.* **2017**, *56*, 15159−15170.

(24) Liu, Y.; Chen, T.; Wong, Y.-S.; Mei, W.-J.; Huang, X.-M.; Yang, F.; Liu, J.; Zheng, W.-J. DNA binding and photocleavage properties and apoptosis-inducing activities of a ruthenium porphyrin complex [(Py-3′) TPP−Ru (phen) 2Cl] Cl and its heterometallic derivatives. *Chem.-Biol. Interact.* **2010**, *183*, 349−356.

(25) Kaushik, N. K.; Mishra, A.; Ali, A.; Adhikari, J. S.; Verma, A. K.; Gupta, R. Synthesis, characterization, and antibacterial and anticancer screening of {M 2+−Co 3+−M 2+} and {Co 3+−M 2+}(M is Zn,

DOI: 10.1021/acs.inorgchem.8b03069
Inorg. Chem. 2019, 58, 2501−2513

Cd, Hg) heterometallic complexes. *JBIC, J. Biol. Inorg. Chem.* **2012**, *17*, 1217−1230.
(26) Boselli, L.; Carraz, M.; Mazères, S.; Paloque, L.; Gonzalez, G.; Benoit-Vical, F.; Valentin, A.; Hemmert, C.; Gornitzka, H. Synthesis, Structures, and Biological Studies of Heterobimetallic Au (I)−Ru (II) Complexes Involving N-Heterocyclic Carbene-Based Multidentate Ligands. *Organometallics* **2015**, *34*, 1046−1055.
(27) González-Pantoja, J. F.; Stern, M.; Jarzecki, A. A.; Royo, E.; Robles-Escajeda, E.; Varela-Ramírez, A.; Aguilera, R. J.; Contel, M. Titanocene−Phosphine Derivatives as Precursors to Cytotoxic Heterometallic TiAu2 and TiM (M= Pd, Pt) Compounds. Studies of Their Interactions with DNA. *Inorg. Chem.* **2011**, *50*, 11099−11110.
(28) Nieto, D.; González-Vadillo, A. M.; Bruña, S.; Pastor, C. J.; Ríos-Luci, C.; León, L. G.; Padrón, J. M.; Navarro-Ranninger, C.; Cuadrado, I. Heterometallic platinum (II) compounds with β-aminoethylferrocenes: synthesis, electrochemical behaviour and anticancer activity. *Dalton Trans.* **2012**, *41*, 432−441.
(29) Lease, N.; Vasilevski, V.; Carreira, M.; de Almeida, A.; Sanaú, M.; Hirva, P.; Casini, A.; Contel, M. Potential anticancer heterometallic Fe−Au and Fe−Pd agents: initial mechanistic insights. *J. Med. Chem.* **2013**, *56*, 5806−5818.
(30) Fernández-Gallardo, J.; Elie, B. T.; Sulzmaier, F. J.; Sanaú, M.; Ramos, J. W.; Contel, M. Organometallic Titanocene−Gold Compounds as Potential Chemotherapeutics in Renal Cancer. Study of their Protein Kinase Inhibitory Properties. *Organometallics* **2014**, *33*, 6669−6681.
(31) Govender, P.; Lemmerhirt, H.; Hutton, A. T.; Therrien, B.; Bednarski, P. J.; Smith, G. S. First-and second-generation heterometallic dendrimers containing ferrocenyl−ruthenium (II)−arene motifs: synthesis, structure, electrochemistry, and preliminary cell proliferation studies. *Organometallics* **2014**, *33*, 5535−5545.
(32) Fernández-Gallardo, J.; Elie, B. T.; Sadhukha, T.; Prabha, S.; Sanaú, M.; Rotenberg, S. A.; Ramos, J. W.; Contel, M. Heterometallic titanium−gold complexes inhibit renal cancer cells in vitro and in vivo. *Chem. Sci.* **2015**, *6*, 5269−5283.
(33) Nieto, D.; Bruña, S.; González-Vadillo, A. M.; Perles, J.; Carrillo-Hermosilla, F.; Antiñolo, A.; Padrón, J. M.; Plata, G. B.; Cuadrado, I. Catalytically generated ferrocene-containing guanidines as efficient precursors for new redox-active heterometallic platinum (II) complexes with anticancer activity. *Organometallics* **2015**, *34*, 5407−5417.
(34) Mui, Y. F.; Fernández-Gallardo, J.; Elie, B. T.; Gubran, A.; Maluenda, I.; Sanaú, M.; Navarro, O.; Contel, M. Titanocene−gold complexes containing N-heterocyclic carbene ligands inhibit growth of prostate, renal, and colon cancers in vitro. *Organometallics* **2016**, *35*, 1218−1227.
(35) Bjelosevic, H.; Guzei, I. A.; Spencer, L. C.; Persson, T.; Kriel, F. H.; Hewer, R.; Nell, M. J.; Gut, J.; van Rensburg, C. E. J.; Rosenthal, P. J. Platinum (II) and gold (I) complexes based on 1, 1′-bis (diphenylphosphino) metallocene derivatives: Synthesis, characterization and biological activity of the gold complexes. *J. Organomet. Chem.* **2012**, *720*, 52−59.
(36) Ferraro, G.; Petruk, G.; Maiore, L.; Pane, F.; Amoresano, A.; Cinellu, M. A.; Monti, D. M.; Merlino, A. Caged noble metals: Encapsulation of a cytotoxic platinum (II)-gold (I) compound within the ferritin nanocage. *Int. J. Biol. Macromol.* **2018**, *115*, 1116−1121.
(37) Ma, L.; Ma, R.; Wang, Z.; Yiu, S.-M.; Zhu, G. Heterodinuclear Pt (iv)−Ru (ii) anticancer prodrugs to combat both drug resistance and tumor metastasis. *Chem. Commun.* **2016**, *52*, 10735−10738.
(38) Madeira, J. M.; Gibson, D. L.; Kean, W. F.; Klegeris, A. The biological activity of auranofin: implications for novel treatment of diseases. *Inflammopharmacology* **2012**, *20*, 297−306.
(39) Elie, B. T.; Pechenyy, Y.; Uddin, F.; Contel, M. A heterometallic ruthenium−gold complex displays antiproliferative, antimigratory, and antiangiogenic properties and inhibits metastasis and angiogenesis-associated proteases in renal cancer. *JBIC, J. Biol. Inorg. Chem.* **2018**, *23*, 399−411.
(40) Bertrand, B.; Citta, A.; Franken, I. L.; Picquet, M.; Folda, A.; Scalcon, V.; Rigobello, M. P.; Le Gendre, P.; Casini, A.; Bodio, E. Gold (I) NHC-based homo-and heterobimetallic complexes: synthesis, characterization and evaluation as potential anticancer agents. *JBIC, J. Biol. Inorg. Chem.* **2015**, *20*, 1005−1020.
(41) Massai, L.; Fernández-Gallardo, J.; Guerri, A.; Arcangeli, A.; Pillozzi, S.; Contel, M.; Messori, L. Design, synthesis and characterisation of new chimeric ruthenium (II)−gold (I) complexes as improved cytotoxic agents. *Dalton Trans.* **2015**, *44*, 11067−11076.
(42) Fernández-Gallardo, J.; Elie, B. T.; Sanaú, M.; Contel, M. Versatile synthesis of cationic N-heterocyclic carbene−gold (I) complexes containing a second ancillary ligand. Design of heterobimetallic ruthenium−gold anticancer agents. *Chem. Commun.* **2016**, *52*, 3155−3158.
(43) Mosmann, T. Rapid colorimetric assay for cellular growth and survival: application to proliferation and cytotoxicity assays. *J. Immunol. Methods* **1983**, *65*, 55−63.
(44) Batchelor, L. K.; Păunescu, E.; Soudani, M.; Scopelliti, R.; Dyson, P. J. Influence of the Linker Length on the Cytotoxicity of Homobinuclear Ruthenium (II) and Gold (I) Complexes. *Inorg. Chem.* **2017**, *56*, 9617−9633.
(45) Timerbaev, A. R.; Pawlak, K.; Gabbiani, C.; Messori, L. Recent progress in the application of analytical techniques to anticancer metallodrug proteomics. *TrAC, Trends Anal. Chem.* **2011**, *30*, 1120−1138.
(46) Lee, R. F. S.; Menin, L.; Patiny, L.; Ortiz, D.; Dyson, P. J. Versatile Tool for the Analysis of Metal−Protein Interactions Reveals the Promiscuity of Metallodrug−Protein Interactions. *Anal. Chem.* **2017**, *89*, 11985−11989.
(47) Messori, L.; Merlino, A. Protein metalation by metal-based drugs: X-ray crystallography and mass spectrometry studies. *Chem. Commun.* **2017**, *53*, 11622−11633.
(48) Quan, L.; Liu, M. CID, ETD and HCD fragmentation to study protein post-translational modifications. *ModChemAppl.* **2013**, *1*, 1−5.
(49) Zhurov, K. O.; Fornelli, L.; Wodrich, M. D.; Laskay, Ü. A.; Tsybin, Y. O. Principles of electron capture and transfer dissociation mass spectrometry applied to peptide and protein structure analysis. *Chem. Soc. Rev.* **2013**, *42*, 5014−5030.
(50) Murray, B. S.; Menin, L.; Scopelliti, R.; Dyson, P. J. Conformational control of anticancer activity: the application of arene-linked dinuclear ruthenium (II) organometallics. *Chem. Sci.* **2014**, *5*, 2536−2545.
(51) Patiny, L.; Borel, A. ChemCalc: a building block for tomorrow's chemical infrastructure. *J. Chem. Inf. Model.* **2013**, *53*, 1223−1228.
(52) Tönnemann, J.; Risse, J.; Grote, Z.; Scopelliti, R.; Severin, K. Efficient and Rapid Synthesis of Chlorido-Bridged Half-Sandwich Complexes of Ruthenium, Rhodium, and Iridium by Microwave Heating. *Eur. J. Inorg. Chem.* **2013**, *2013*, 4558−4562.
(53) Uson, R.; Laguna, A. Polyaryl Derivatives of gold (I), silver (I) and gold (III), *Organomet. Synth* **1986**, *3*, 322−342.

DOI: 10.1021/acs.inorgchem.8b03069
Inorg. Chem. 2019, 58, 2501−2513